

STARS

From stellar models to nucleosynthesis

Oscar Straniero

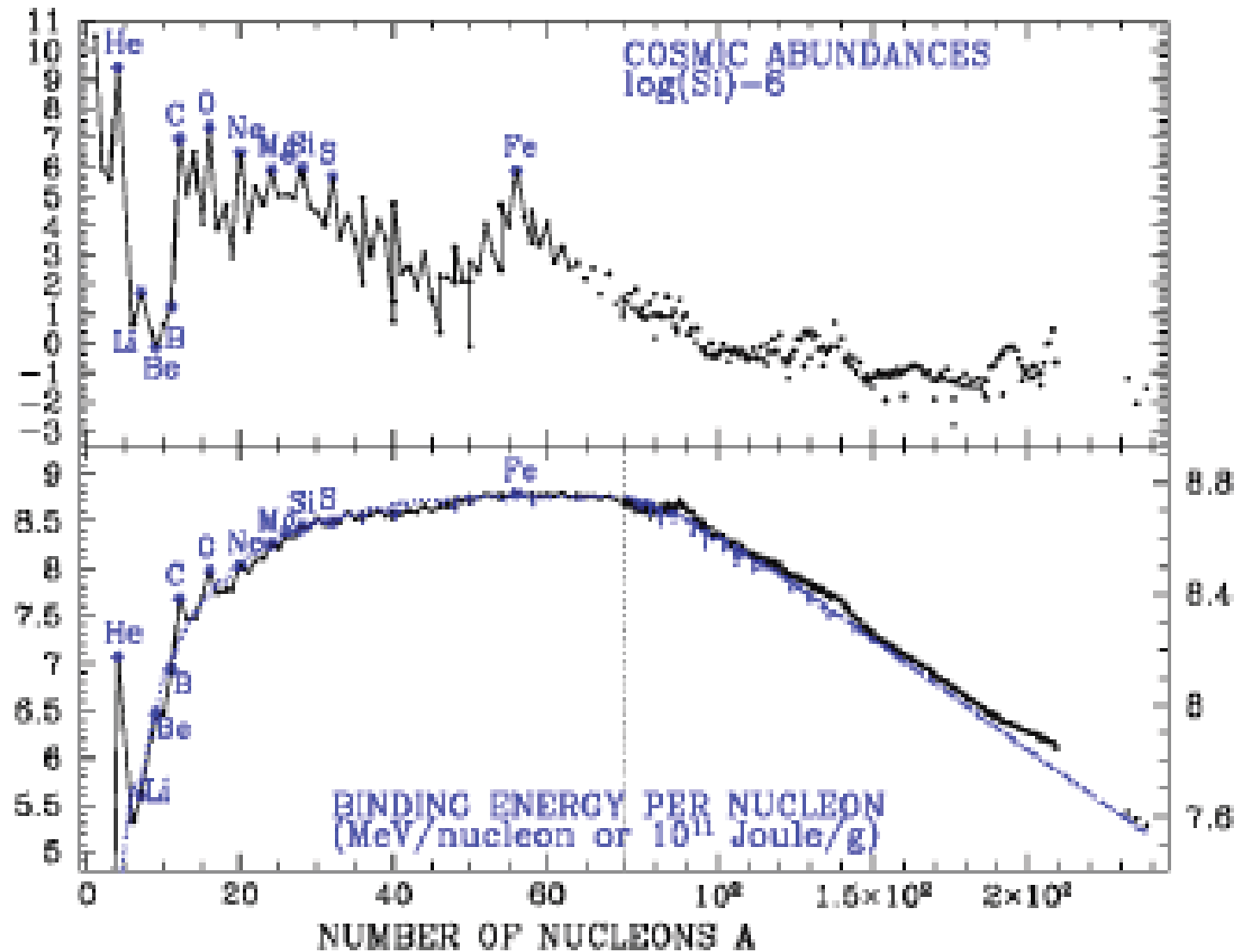
Italian National Institute of Astrophysics

The n_TOF nuclear physics winter school, gen 21-24, 2024

OVERVIEW:

- Stellar models and nucleosynthesis, a brief introduction.
- Nuclear reactions in stars
- Evolution of low-mass stars.
- The Asymptotic Giant Branch.
- Synthesis of elements beyond the iron peak in AGB stars .
- The origin of the main s-process component.

Binding energy per nucleon E_B/A is **maximum** for ^{56}Fe



$S(E)$ of the $^{12}\text{C}+^{12}\text{C}$ reaction. High energy data show a series of narrow resonances, representing a clustered structure (α clusters) of the compound nucleus of $^{24}\text{Mg}^*$.

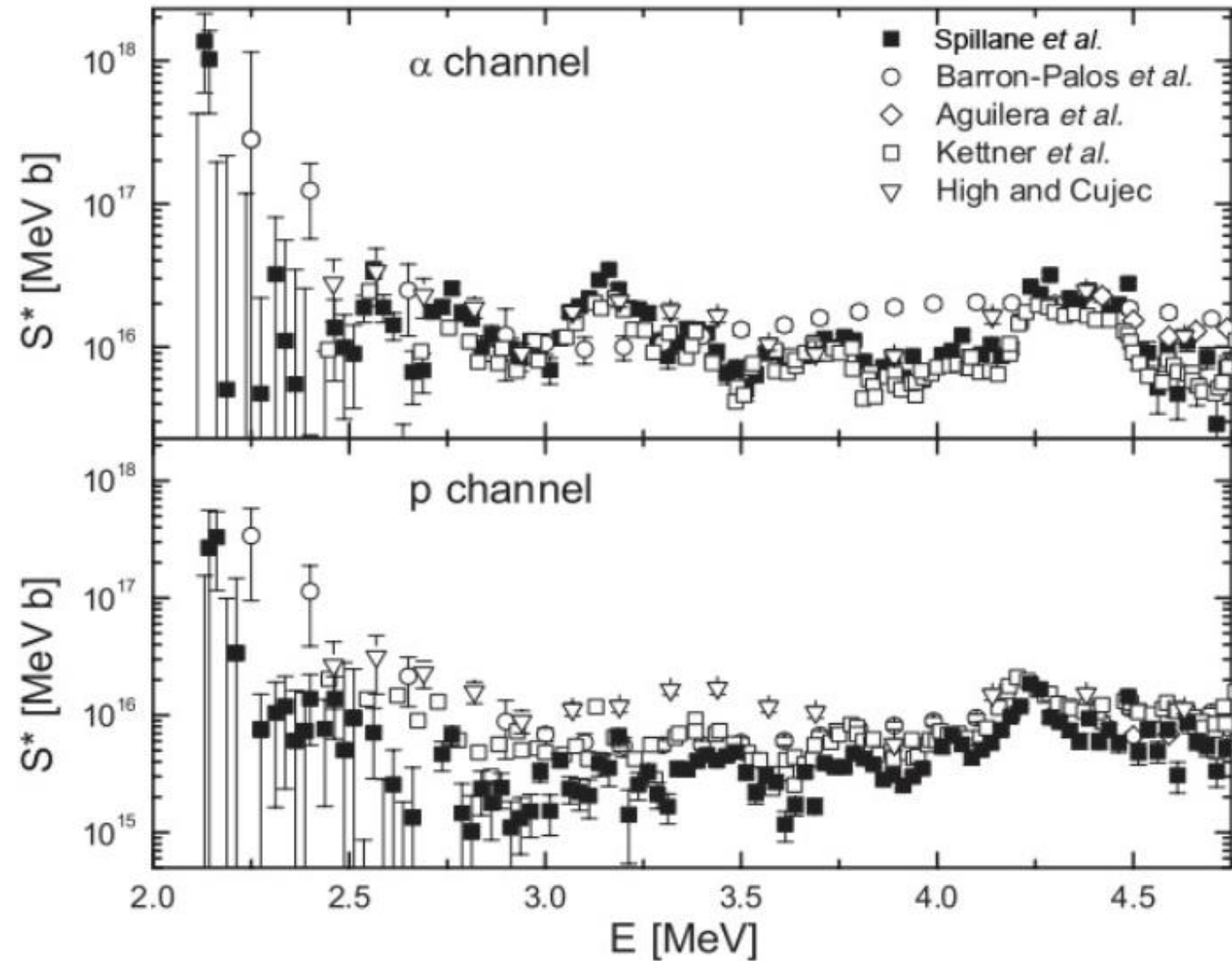


Figure 3.4: \tilde{S} -factor of the $^{12}\text{C}+^{12}\text{C}$ reactions obtained by five different groups using gamma-ray spectroscopy. The discrepancy between data sets in certain energy regions is not yet understood. Low energy data is governed by large uncertainties due to the H contamination in the targets. Figure taken from [44].

A stellar model may be as complex as you want: rotation, magnetic fields, dynamical and secular instabilities of various nature,

However, most of our knowledge concerning stellar evolution is based on relatively simple models: **Self-gravitating, spherical symmetric stars in thermal and hydrostatic equilibrium.**

STELLAR STRUCTURE EQUATIONS:

$$\frac{dP}{dm_r} = -\frac{GM_r}{4\pi r^4} \quad \text{Hydrostatic equilibrium}$$

$$\frac{dr}{dm_r} = \frac{1}{4\pi r^2 \rho} \quad \text{Mass conservation}$$

$$\frac{dL_r}{dm_r} = \varepsilon_{nucl} - \varepsilon_\nu + \varepsilon_{grav} \quad \text{Energy conservation}$$

$$\frac{dT}{dm_r} = -\nabla \frac{GM_r}{4\pi r^4} \frac{T}{P} \quad \text{Energy transport}$$

$$\frac{dY_i}{dt} = \left(\frac{dY_i}{dt} \right)_{nuc} + \left(\frac{dY_i}{dt} \right)_{mix} \quad i = 1, \dots, N$$

Nuclear reactions + turbulent convection

Spatial & temporal resolution:

1 stellar model contains about 1000 mesh points: $m_r=0$ to M

1 evolutionary track contains up to 10^6 stellar models: from $t = 0$ to 13 Gyr or collapse

The overall problem: 4+N differential equations, in 4+N dependent variables:

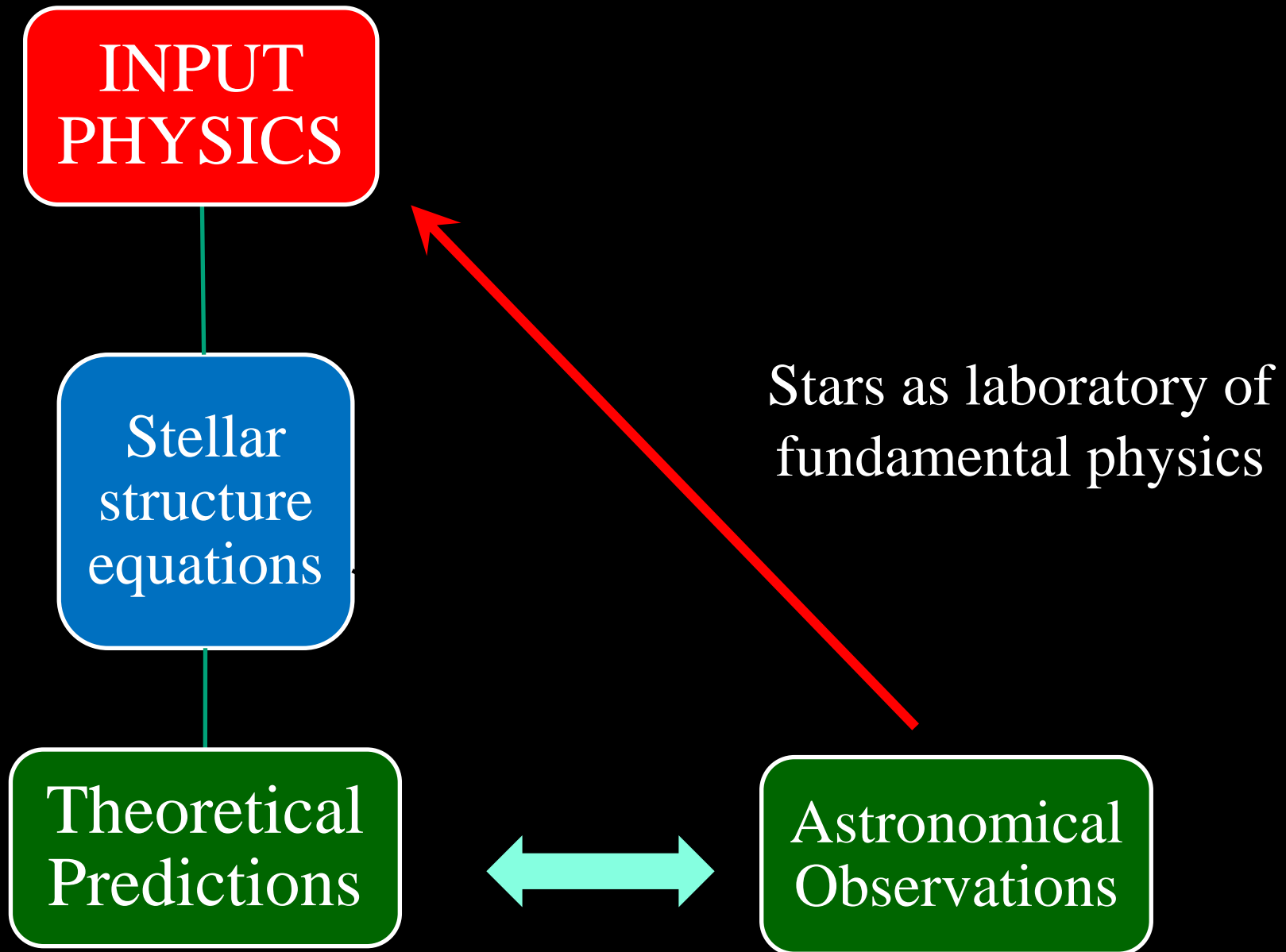
- r (radius),
- L_r (luminosity),
- P (pressure),
- T (temperature),
- Y_i (chemical composition: abundances)

all depending on the lagrangian mass coordinate:

$$m_r = \int_0^r 4\pi \rho r^2 dr$$

and the time: t

*Appropriate boundary conditions needed



a STAR evolves because:

- 1. Energy loss, as due to photons and neutrinos emission.**
- 2. Chemical composition changes, as due to the concurrent action of nuclear burning and mixing.**

Energy leaks....

$$\varepsilon_\gamma = \text{radiation} = \frac{dL_r}{dm_r}$$

$$\varepsilon_\nu = \text{plasma} + \text{bremsstrahlung} + \text{compton} + \text{pair}$$

.....Energy sources

$$\mu_i = \left(\frac{\partial E}{\partial N_i} \right)_{S, \rho, N_{j \neq i}} \quad \text{chemical potential}$$

$$\varepsilon_{\text{grav}} = -T \frac{dS}{dt} = -\frac{dE}{dt} + \frac{P}{\rho^2} \frac{d\rho}{dt} - \sum_i \mu_i \frac{dN_i}{dt}$$

$$\varepsilon_{\text{nucl}} = \sum_k Y_i Y_j \rho N_A \langle \sigma v \rangle_k Q_k$$

$$\langle \sigma v \rangle_k = \left(\frac{8}{\pi \mu} \right)^{1/2} \left(\frac{1}{KT} \right)^{3/2} \int_0^\infty \sigma(E) E e^{-\frac{E}{KT}} dE$$

$$N_j = \rho N_A Y_j$$

From energy conservation

$$L = \int_0^M (\varepsilon_{nucl} + \varepsilon_{grav} + \varepsilon_v) dm_r = 4\pi R^2 \sigma T_{eff}^4$$

T_{eff} = effective temperature

surface temperature if stars were perfect black bodies

Roughly speaking, it corresponds to the temperature at the base of the photosphere

composition changes

$$Y_i = X_i / A_i$$

$$\frac{dY_i}{dt} = \left(\frac{dY_i}{dt} \right)_{nuc} + \left(\frac{dY_i}{dt} \right)_{mix} \quad i = 1, \dots, N$$

$$\left(\frac{dY_i}{dt} \right)_{nuc} = \sum_j c_i(j) \lambda_j Y_i + \sum_{j,k} c_i(j,k) \rho N_A \langle \sigma v \rangle_{j,k} Y_j Y_k + \sum_{j,k,l} c_i(j,k,l) \rho^2 N_A^2 \langle \sigma v \rangle_{j,k,l} Y_j Y_k Y_l \quad \text{nuclear}$$

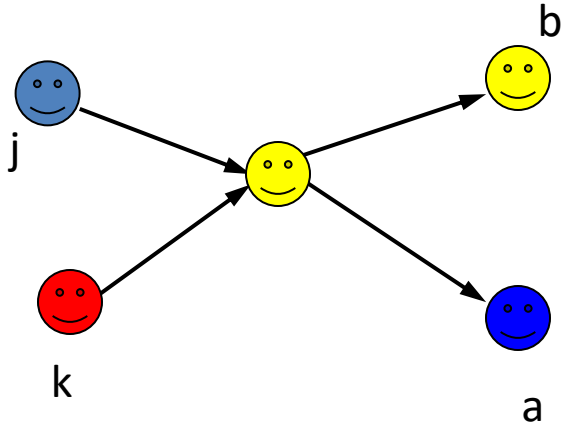
$$\left(\frac{dY_i}{dt} \right)_{mix} = \frac{\partial}{\partial r} D \frac{\partial Y_i}{\partial r} - \mathbf{v} \frac{\partial Y_i}{\partial r}$$

Mixing: dynamical or secular instabilities

Nuclear reactions in an astrophysical PLASMA

- In stellar interiors, nuclei are in thermal equilibrium with electrons and photons.
- At variance with the electrons, their thermal energy spectrum is always well described by the classical Maxwell-Boltzmann distribution (with rare exceptions, such as in the case of a neutron stars). Nuclear masses are much larger than the electron mass, indeed!!!

Nuclear reaction: fusion of 2 nuclei



Center of mass energy

density of pair with CM energy E

$$v = |v_j - v_k|$$

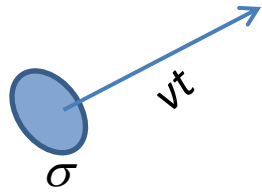
$$\mu = \frac{m_j m_k}{m_j + m_k} = \frac{A_j A_k}{A_j + A_k} m_H$$

$$E = \frac{1}{2} \mu v^2$$

$$n_{jk} = \frac{n_j n_k}{1 + \delta_{jk}}$$

A factor $\frac{1}{2}$ is needed in case of identical nuclei

Reaction Rate



σ is the cross section

$f(\mathbf{v})$ is the velocity distribution function

the rate of reactions among particles pairs with relative velocity between \mathbf{v} and $\mathbf{v}+d\mathbf{v}$:

Equation 1

$$\textit{specific reaction rate} = \frac{n_j n_k}{1 + \delta_{jk}} \sigma v f(v) d^3 v$$

since $d^3v=4\pi v^2 dv$ and $E= \frac{1}{2} \mu v^2$, and using the MB energy distribution:

$$f(v)4\pi v^2 dv = \frac{2}{\sqrt{\pi}} \frac{E^{1/2} e^{-E/kT}}{(kT)^{3/2}} dE.$$

Substituting into equation 1:

$$SRR = \frac{n_j n_k}{1 + \delta_{jk}} \sigma \left(\frac{2E}{\mu} \right)^{\frac{1}{2}} f(v) d^3v = \frac{n_j n_k}{1 + \delta_{jk}} \sigma \left(\frac{8}{\pi \mu} \right)^{\frac{1}{2}} \frac{E e^{-\frac{E}{KT}}}{(KT)^{3/2}} dE$$

This is the n. of reaction among pairs with energy E e $E+dE$. Note that it depends on T , on the density of the interacting nuclei and on the energy.

To get the *total reaction rate*, we must integrate over the whole energy spectrum

Total rate: Integral over the energy spectrum:

$$R_{jk} = \frac{1}{1 + \delta_{jk}} n_j n_k \int_0^{\infty} \sigma(E) \left(\frac{2E}{\mu} \right)^{\frac{1}{2}} f(E) dE$$

$$\langle \sigma v \rangle_{jk} = \left(\frac{8}{\pi \mu} \right)^{1/2} \left(\frac{1}{KT} \right)^{3/2} \int_0^{\infty} \sigma(E) E e^{-\frac{E}{KT}} dE$$

Equation 2

$$n_j = \frac{\rho N_A X_j}{A_j} \quad X_j, \text{ mass fraction; } \rho, \text{ mass density}$$

$$R_{jk} = \frac{1}{1 + \delta_{jk}} \frac{X_j X_k}{A_j A_k} \rho^2 N_A^2 \langle \sigma v \rangle_{jk}$$

Equation 3

Reaction Rate = Number of reaction/time/volume

What about the cross section?

Nuclear reactions among charge nuclei

- Thermal energy should be large enough to allow nuclei penetrate the Coulomb barrier.

$$\frac{Z_1 Z_2 e^2}{r_0} \sim 1.4 Z_1 Z_2 \text{ MeV}$$

Classically, $T \sim 10^{10} \text{ K}$

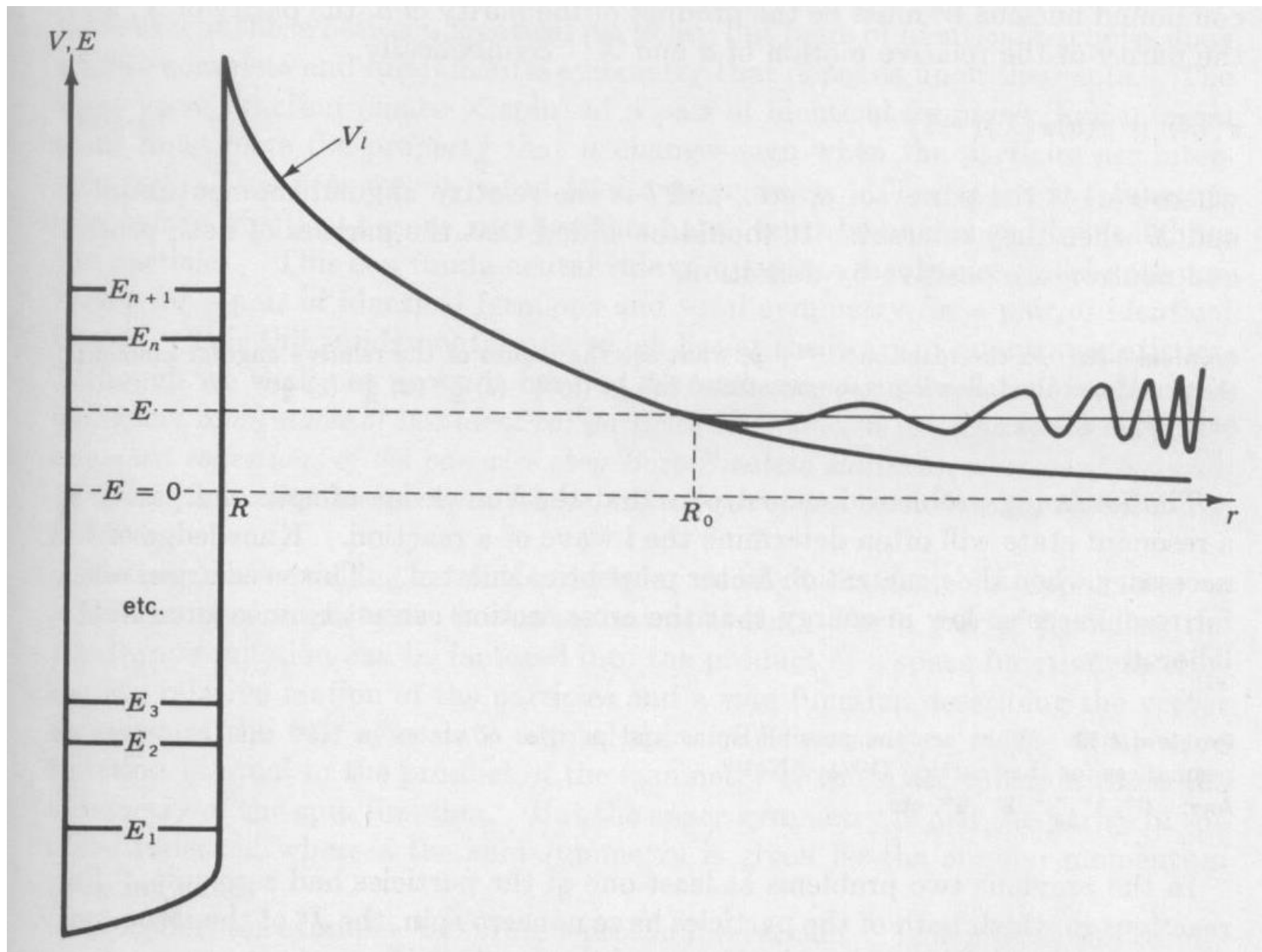
In normal stars temperatures are much lower. keV, rather than MeV. For instance, the central temperature of the Sun is $\sim 10^7 \text{ K}$

Nuclear fusion: cross section

The cross section $\sigma(E)$ represents the probability that a reaction occurs among particle pairs with center-of-mass energy = E. It is the product of 2 independent probabilities representing:

- a) The penetration of Coulomb barrier (**Coulomb probability**)
- b) The formation of a specific the compound nucleus (**nuclear probability**)

$$\sigma(E) = P_{Cou} P_{nuc}$$



The penetrability of the Coulomb barrier:

- The Coulomb barrier is too high, but quantum mechanics allows its penetrability.

The tunnel probability is (Gamow 1934):

$$P_{Coul} = \exp\left(-\frac{2\pi Z_j Z_k e^2}{\hbar v}\right) = \exp\left(-\frac{\sqrt{2}\pi Z_j Z_k e^2}{\hbar} \left(\frac{\mu}{E}\right)^{1/2}\right)$$

$$P_{Coul} = \exp\left(-\frac{b}{\sqrt{E}}\right)$$

- For non-resonant reactions, $P_{nuc}(E)$ is a slowly decreasing function of E:

$$P_{nuc}(E) \approx \pi\lambda^2 \propto \left(\frac{1}{p}\right)^2 \propto \frac{1}{E} \quad \lambda = \frac{h}{p}$$

- So, introducing the ***astrophysical factor*** $S(E)$

$$P_{nuc}(E) = \frac{S(E)}{E}$$

For non-resonant reactions, $S(E)$ is a slowly varying function of E.

- The cross section is the product of the **tunnel probability** and a **nuclear probability**:

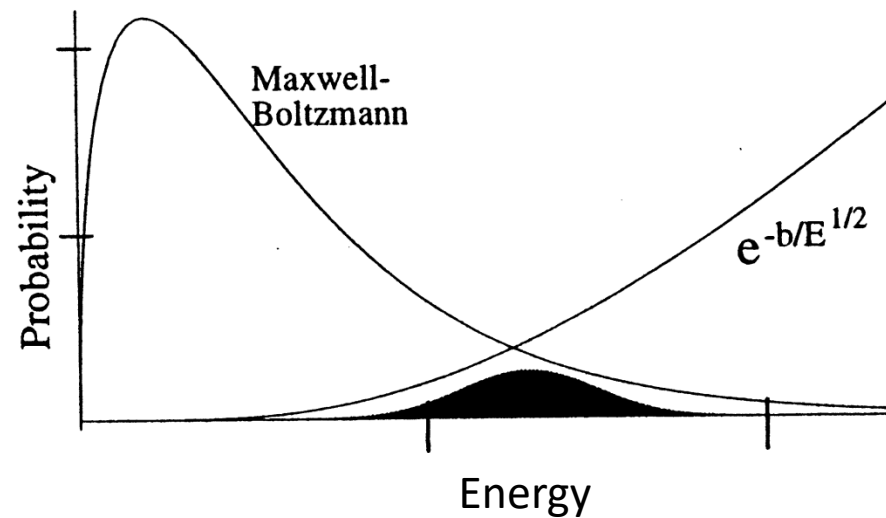
$$\sigma(E) = \frac{1}{E} S(E) \exp\left(-\frac{b}{E^{1/2}}\right)$$

$$b = \frac{\sqrt{2}\pi Z_j Z_k e^2 \mu^{1/2}}{\hbar} = 0.99 Z_j Z_k \mu^{1/2} \text{ MeV}^{1/2}$$

The Gamow's peak

- After substitutions:

$$\langle \sigma v \rangle = \left(\frac{8}{\pi \mu} \right)^{1/2} \frac{1}{(kT)^{3/2}} \int_0^{\infty} S(E) \exp \left[-\frac{E}{kT} - \frac{b}{E^{1/2}} \right] dE$$



The maximum occurs at:

$$\frac{d}{dE} \exp\left(-\frac{E}{KT} - \frac{b}{E^{1/2}}\right) = -\exp\left(-\frac{E}{KT} - \frac{b}{E^{1/2}}\right) * \left(\frac{1}{KT} - \frac{b}{2} E^{-\frac{3}{2}}\right) = 0$$

$$E_0 = \left(\frac{bKT}{2}\right)^{\frac{2}{3}}$$



GAMOW's Peak

$$E_0 = 1.22 \times (\beta T_6^2)^{1/3} \text{ KeV}$$

$$\beta = Z_j^2 Z_k^2 A_\mu$$

$$A_\mu = \frac{\mu}{m_H} = \frac{A_j A_k}{A_j + A_k} \quad \text{and} \quad T_6 = T/10^6 \text{ K}$$

Gamow's peak energy in different astrophysical environments:

T = 1 GK (Universe, 3 m after BB)

p+d 100 KeV

T = 16 MK (Sun)

p+p 5 KeV

3He+3He 20 KeV

3He+4He 21 KeV

14N+p 25 KeV

T = 70 MK (RGB stars)

14N+p 65 KeV

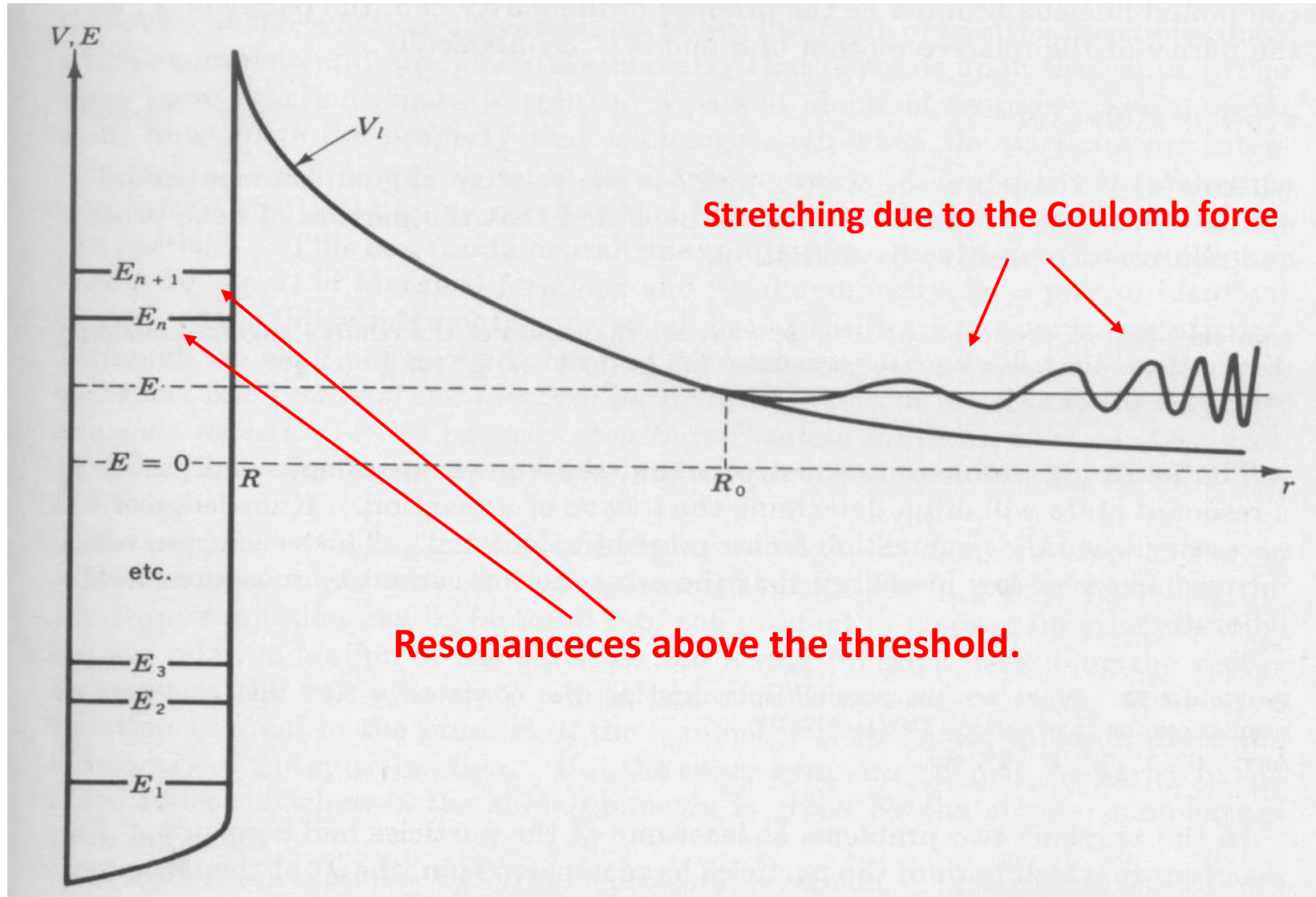
T = 200 MK (He-burning)

12C+ α 300 KeV

T = 600 MK (C-burning)

12C+12C 1.5 MeV

Resonances





Eugene Wigner
(1902-95)
Nobel Prize 1963

The cross section contribution due to a single resonance is given by the Breit-Wigner formula:

$$\sigma(E) = \pi \hat{\lambda}^2 \cdot \omega \cdot \frac{\Gamma_1 \Gamma_2}{(E - E_r)^2 + (\Gamma / 2)^2}$$

Usual geometric factor
 $= \frac{0.656}{\hat{A}} \frac{1}{E}$ barn

Spin factor:
 $\omega = \frac{2J_r + 1}{(2J_1 + 1)(2J_2 + 1)}$

$\propto \Gamma_1$ Partial width for decay of resonance by emission of particle 1
= Rate for formation of Compound nucleus state

$\propto \Gamma_2$ Partial width for decay of resonance by emission of particle 2
= Rate for decay of Compound nucleus into the right exit channel

Γ = Total width is in the denominator as a large total width reduces the maximum probabilities (on resonance) for decay into specific channels.

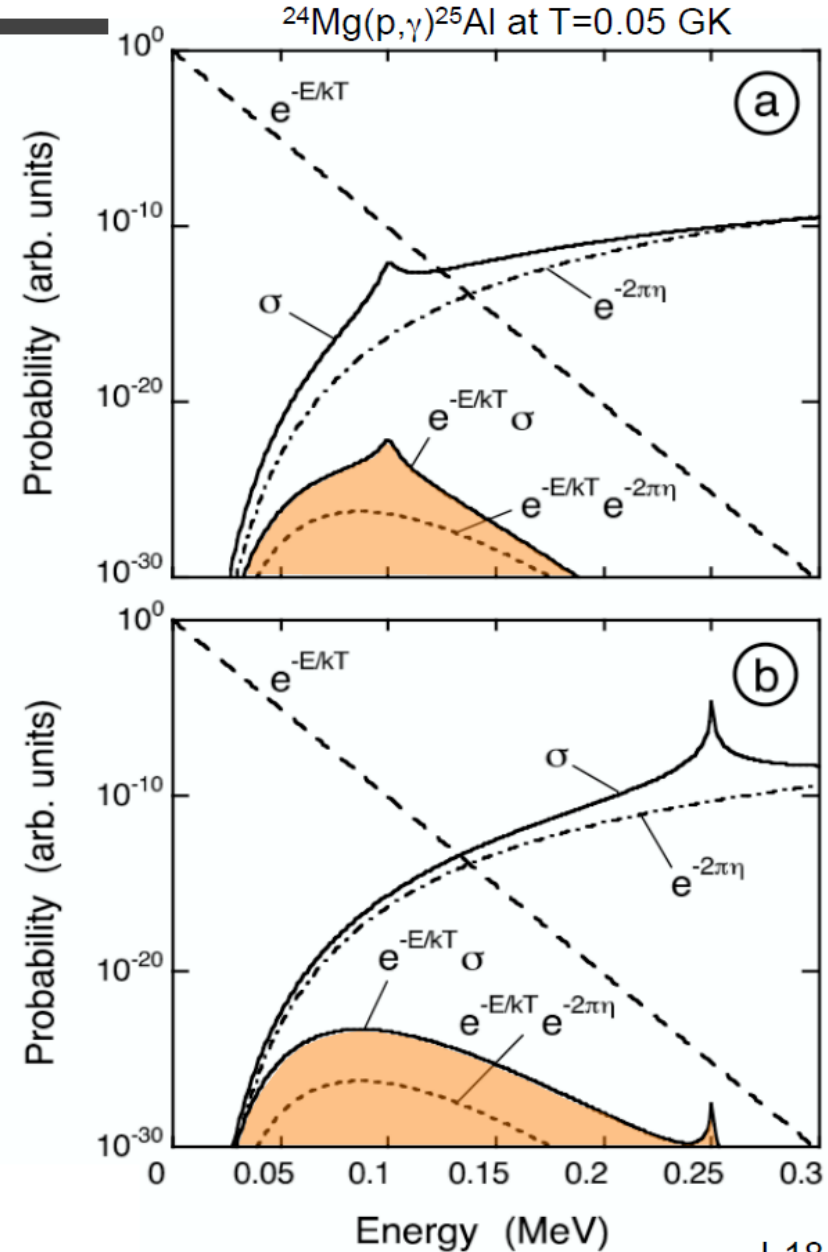
Special case #3: Rates for “Broad Resonances”

Breit-Wigner formula (energy-**dependent** partial widths)

$$N_A \langle \sigma v \rangle = \left(\frac{8}{\pi m_{01}} \right)^{1/2} \frac{N_A}{(kT)^{3/2}} \int_0^\infty E \sigma(E) e^{-E/kT} dE$$

rate can be found from numerical integration

There are two contributions to the rate:
 (i) from “narrow resonance” at E_r
 (ii) from tail of broad resonance



And in case of neutrons?

Rate x unit mass

$$\mathfrak{R}_{jk} = \frac{R_{jk}}{\rho} = \frac{X_j X_k}{A_j A_k (1 + \delta_{jk})} N_a^2 \rho \langle \sigma v \rangle_{jk}$$

Rate of energy production \longrightarrow

$$\mathcal{E}_{Nuclear} = Q_{jK} \mathfrak{R}_{jk}$$

dove

$$Q_{jK} = \Delta mc^2 - E_\nu$$

- Fraction by number:

$$Y_j = \frac{X_j}{A_j}$$

- Two bodies reactions:

$$\mathfrak{R}_{jk} = \frac{1}{j!k!} Y_j Y_k N_a^2 \rho \langle \sigma v \rangle_{jk}$$

- Three bodies (triple- α):

$$\mathfrak{R}_{ijk} = \frac{1}{i!j!k!} Y_i Y_j Y_k N_a^3 \rho^2 \langle \sigma v \rangle_{ijk}$$

- Radioactive decays:

$$n_i(t) = n_i(0) \exp(-\lambda_i t)$$

$\tau_i = e$ -folding time

$$\lambda_i = \frac{1}{\tau_i}$$

$$R_i = \frac{dn_i}{dt} = \pm N_a \rho Y_k \lambda_k \frac{n_i}{A_i} \quad \mathfrak{R}_i = \pm N_a Y_k \lambda_k$$

Chemical changes. General problem!

$$\frac{dY_i}{dt} = \text{productions} - \text{destructions} \quad i=1\dots\dots n$$

$$\frac{dY_i}{dt} = \sum_j c_j^i Y_j N_a \lambda_j + \sum_{jk} c_{jk}^i Y_j Y_k N_a^2 \rho \langle \sigma v \rangle_{jk} + \sum_{jkl} c_{jkl}^i Y_j Y_k Y_l N_a^3 \rho^2 \langle \sigma v \rangle_{jkl}$$

$$c_j^i = \pm 1$$

$$c_{jk}^i = \pm \frac{i}{j!k!} = \pm \frac{i}{1 + \delta_{jk}}$$

$$c_{jkl}^i = \pm \frac{i}{j!k!l!}$$

Notes:

1) n_i is the number of i involved in the reaction.

2) (-) in case $i=k$ or j or l

Libraries of reaction rates ($\text{Na}\langle\sigma v\rangle$)

For reactions among charge nuclei

- REACLIB: <https://reaclib.jinaweb.org/>

For neutron captures:

- KADONIS: <http://www.kadonis.org/>

$^{13}\text{C}(\alpha, n)^{16}\text{O}$

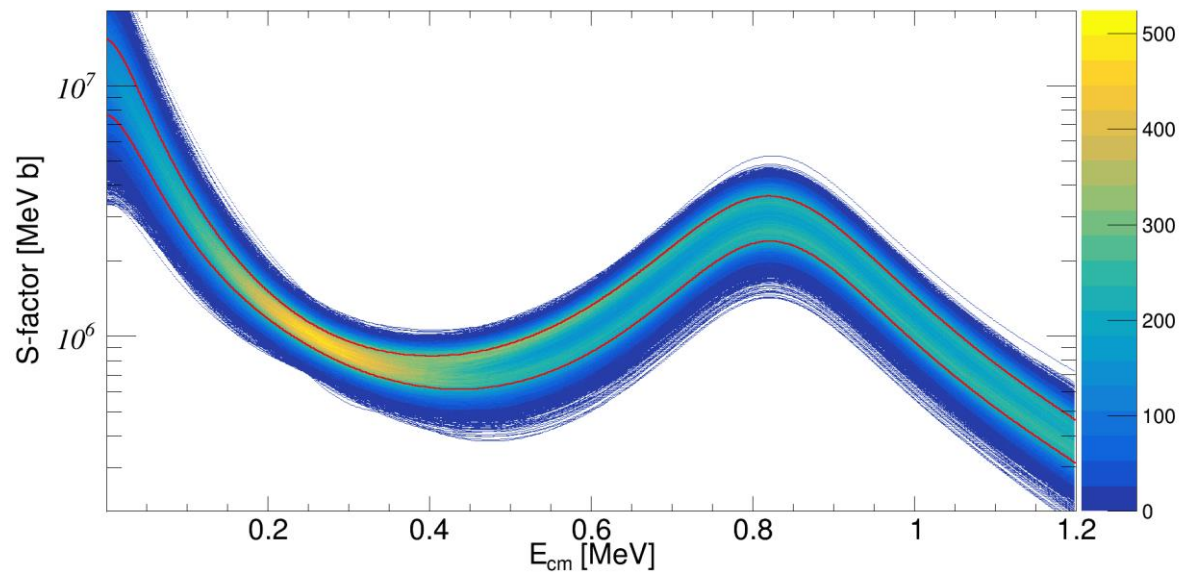
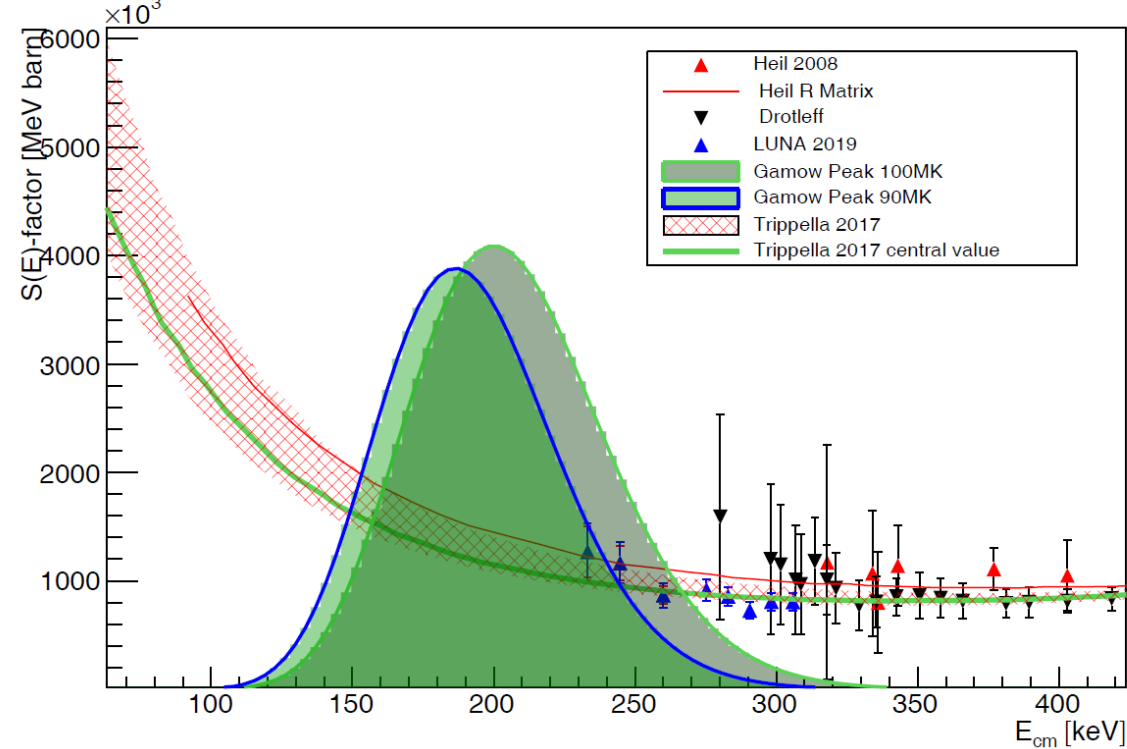
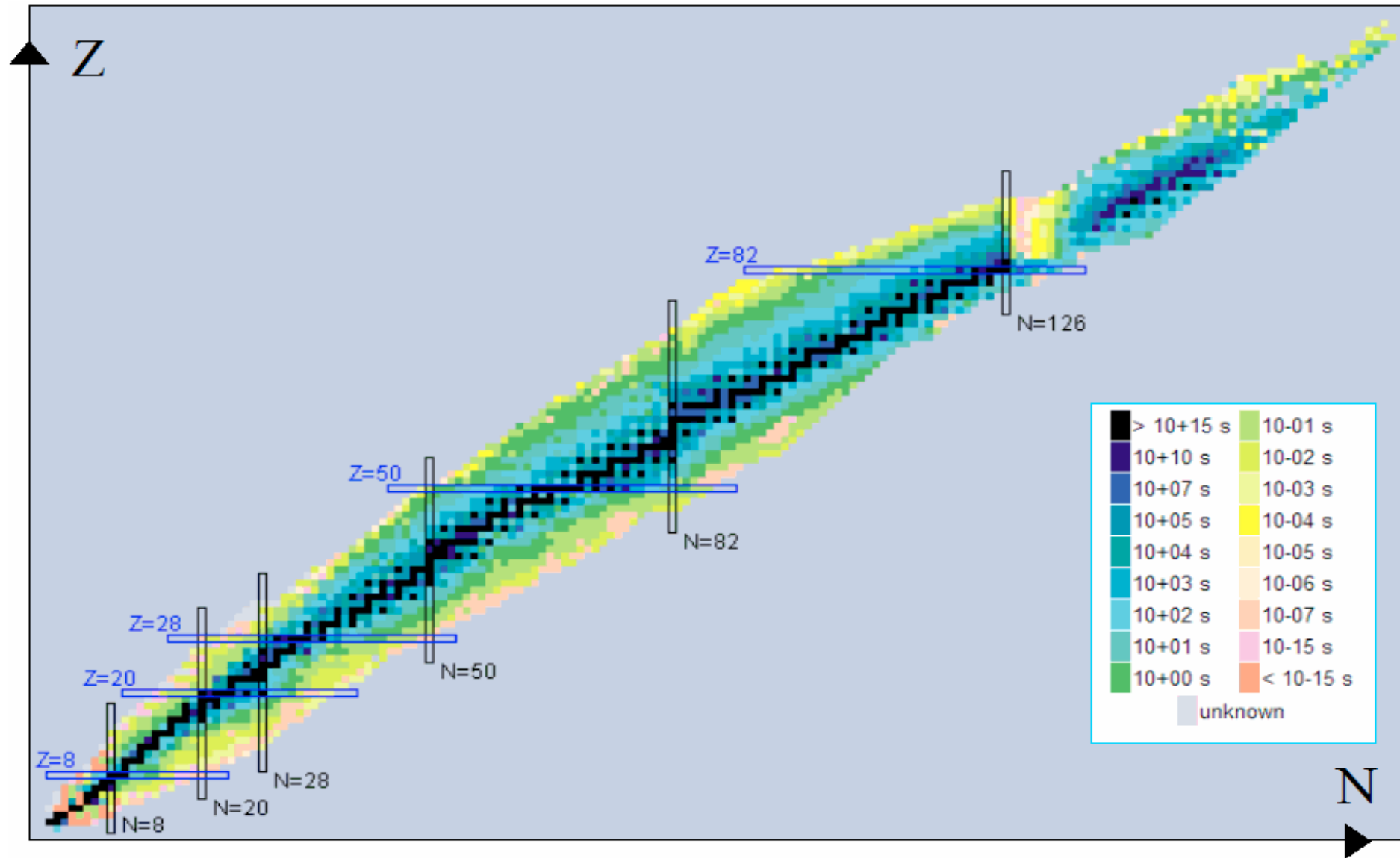


Chart of nuclides (or isotopes)



The nuclear network of a stellar model

- In principle, the network should include all the isotopes that can be produced/consumed.
- For instance, if neutrons are released, as in AGB stars, all the stable isotopes with $1 \leq A \leq 208$ and those unstable, but closer to the stability valley in the n-rich side, should be considered: that is about 600-700 isotopes.....or 600-700 (+4) differential equations.
- In many extant stellar models (but not all), the network is limited to the isotopes involved in nuclear reactions that account for most of the energy generation. Then, a detailed nucleosynthesis is calculated by means of a post-process code.
- However, the selection of the minimal network to be used in stellar model calc is not an obvious task, in particular, when mixing by convection and nuclear burning occur on timescales comparable to the timescale of the physical structure variations. This is a common feature of the advanced phases of stellar evolution.

Energy transport by radiation and
convective instabilities

Energy transport

$$\nabla = \frac{d \ln T}{d \ln P}$$

opacity



$$\nabla_{rad} = \frac{3kr^2 P}{4acGM_r T^4} F = \frac{3kr^2 P}{4acGM_r T^4} \frac{L_r}{4\pi r^2}$$

$$\nabla_{ad} = \frac{\gamma - 1}{\gamma \chi_T} \quad \gamma = \frac{C_P}{C_V} \quad \chi_T = \left(\frac{d \ln P}{d \ln T} \right)_{\rho, Y_i}$$

conv. dominated $\nabla_{ad} \leq \nabla \leq \nabla_{rad}$ rad. dominated

Convective inStability

$$\nabla_{rad} > \nabla_{ad} + \frac{\phi}{\delta} \nabla_{\mu} \quad \text{Convection on}$$

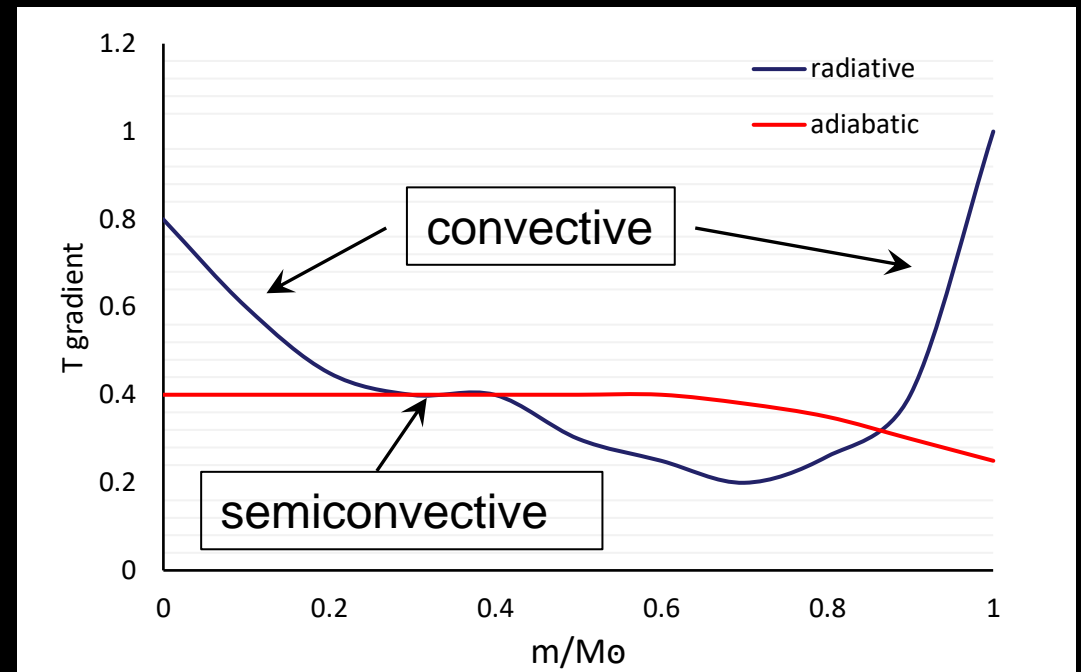
where:

$$\phi = \left(\frac{\partial \ln \rho}{\partial \mu} \right)_{P,T} = 1 \text{ for a perfect gas}$$

$$\delta = \left(\frac{\partial \ln \rho}{\partial T} \right)_{P,\mu} = 1 \text{ for a perfect gas}$$

$$\nabla_{\mu} = \frac{d \ln \mu}{d \ln P} = 0 \text{ for homogeneous layers}$$

Schwarzschild/Ledoux criteria for convective instability



<http://pos.sissa.it/cgi-bin/reader/conf.cgi?confid=148>

<https://link.springer.com/article/10.1140/epjp/i2018-12237-1>



PROCEEDINGS
OF SCIENCE

An introduction to Stellar Evolution

Oscar Straniero¹

INAF-Osservatorio Astronomico di Teramo

Via Maggini s.n.c., 64100 Teramo, Italy

E-mail: straniero@oa-teramo.inaf.it

Stellar evolution theory is among the greatest successes of modern astrophysics. It is a powerful tool to interpret many astronomical observations, such as the Colour-Magnitude diagrams of simple and complex stellar systems or the chemical composition of the stars. Stellar models are required to derive important parameters, like the age of various cosmic components or their distances. In addition, stellar models allow us to investigate the behaviour of matter and radiation in the extreme physical conditions taking place in stellar interiors.

In this lecture, I review the main ingredients needed to *cook* a stellar model. Few examples of the potential of stellar evolution in the interpretation of relevant astronomical observations are illustrated. A final section is devoted to core-He burning stellar models and the interplay between nuclear burning and convection that determines the evolution of many stars.

[Home](#) > [The European Physical Journal Plus](#) > [Article](#)

On the mass of supernova progenitors

Review | [Published: 26 September 2018](#)

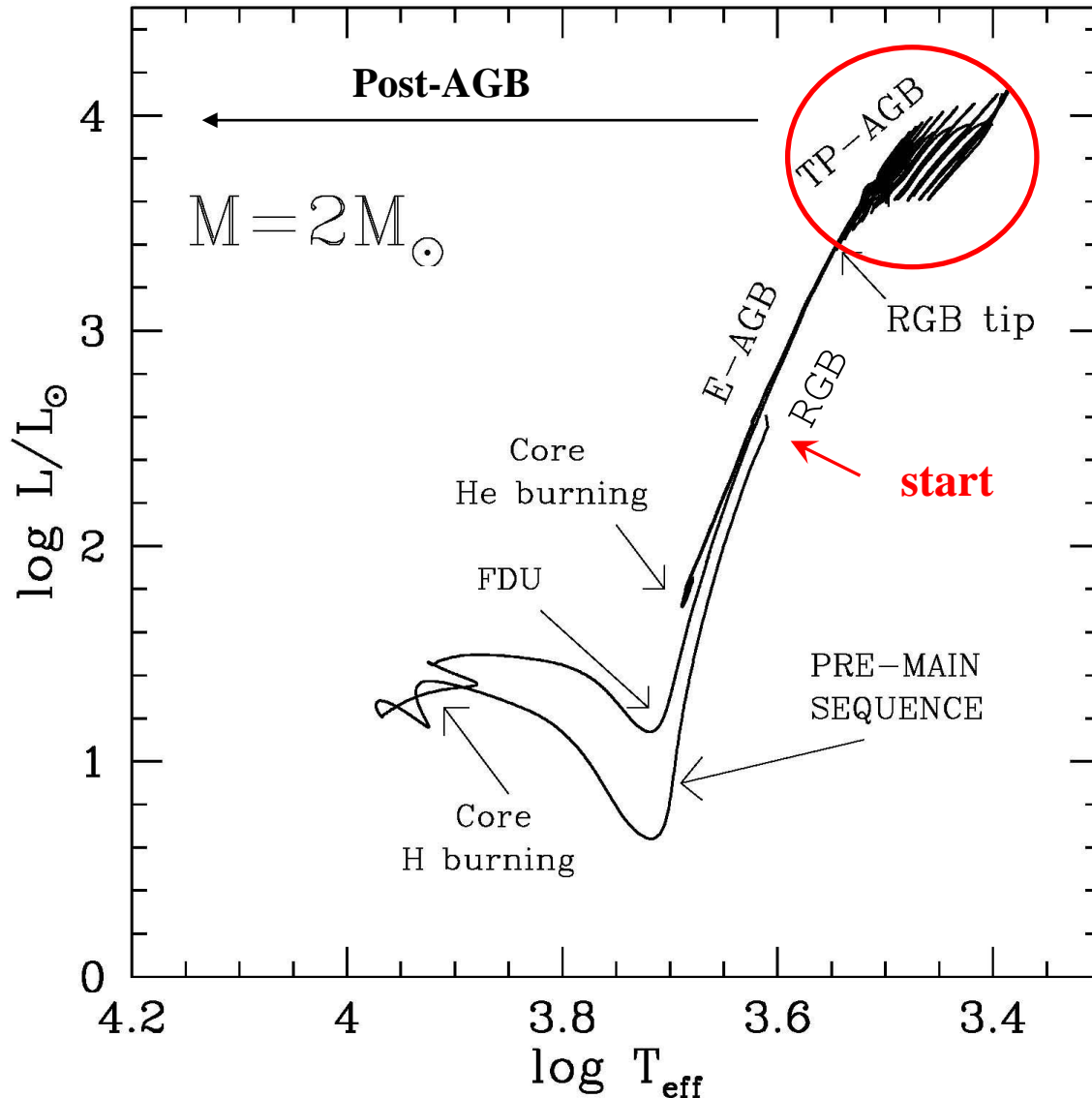
Volume 133, article number 388, (2018) [Cite this article](#)



[The European Physical Journal Plus](#)

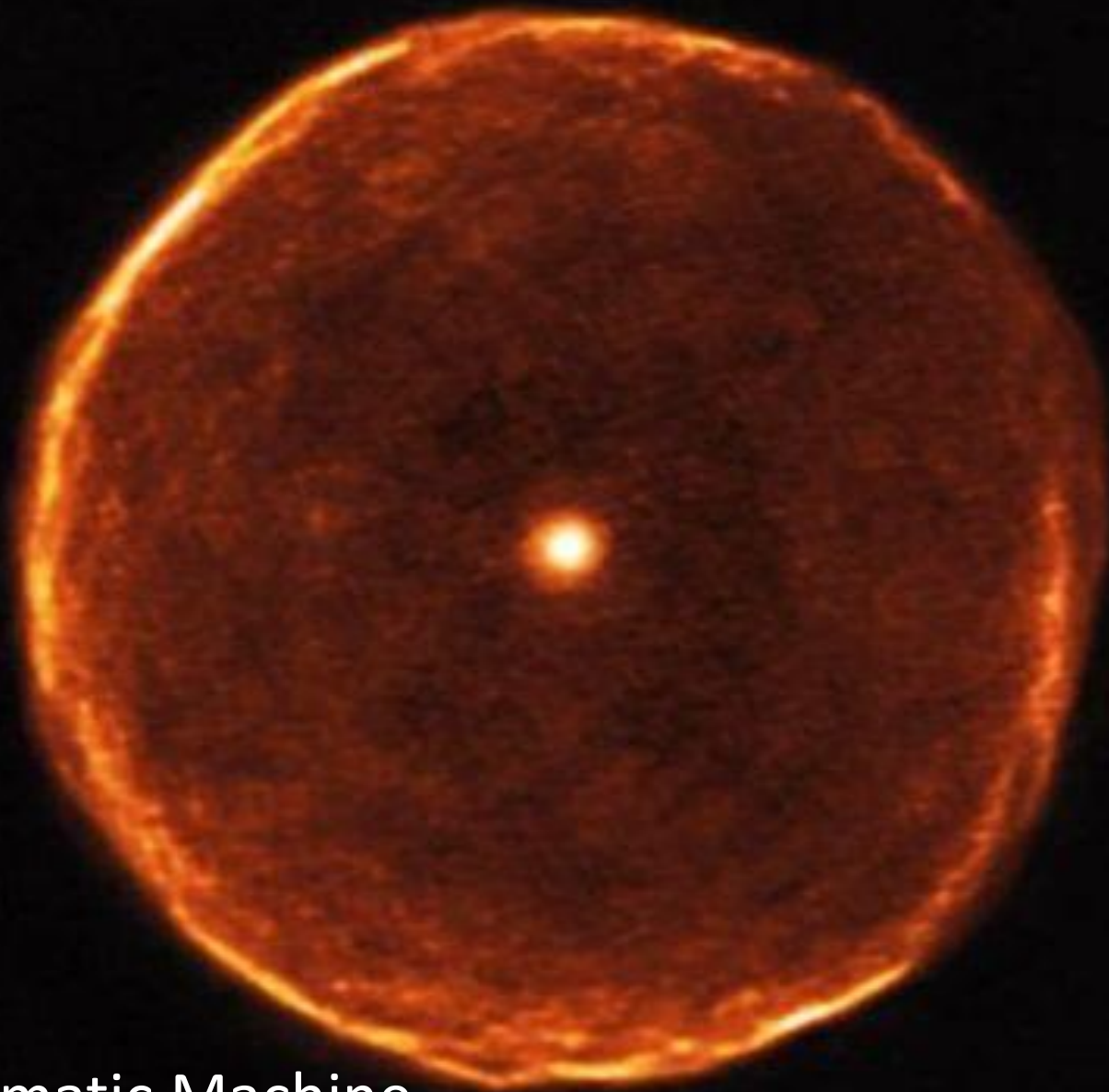
Application to stars

The Hertzsprung-Russell diagram



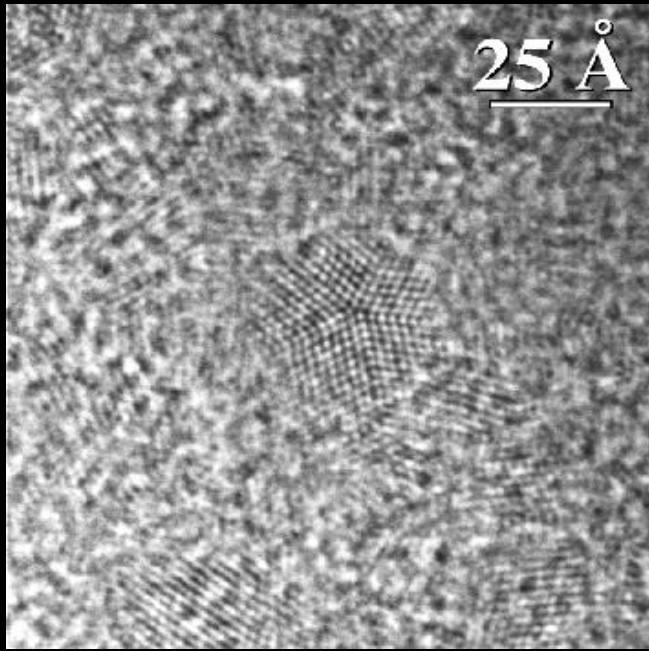
1. Pre-MS → fully convective star (because of large opacity).
2. MS → convective core (powered by H burning through the CNO cycle)
3. FDU (first dredge up) → the envelope cool down and a deep convective envelope develops (due to shell-H burning + large opacity)
4. RGB → degenerate core and deep convective envelope.
5. RGB tip → activation of the triple- α (He-flash)
6. Core-He burning → triple- α followed by $12\text{C} + \alpha$, fully convective core surrounded by a semiconvective layer (where partial mixing of He, C and O allows neutrality).
7. Early-AGB → two burning shell (H and He) → deep convective envelope (large opacity).
8. Thermal Pulse AGB → Alternate shell burnings, deep convective envelope periodically penetrating the H-exhausted core – when H burning off (third dredge up or TDU)

Asymptotic Giant Branch stars

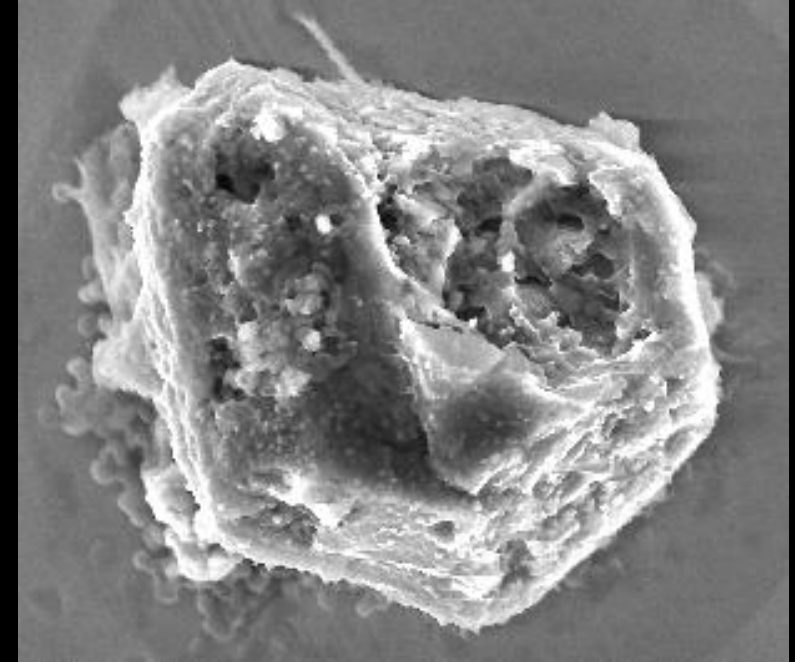


U Antliae in the Pneumatic Machine

STURDUST



Diamonds

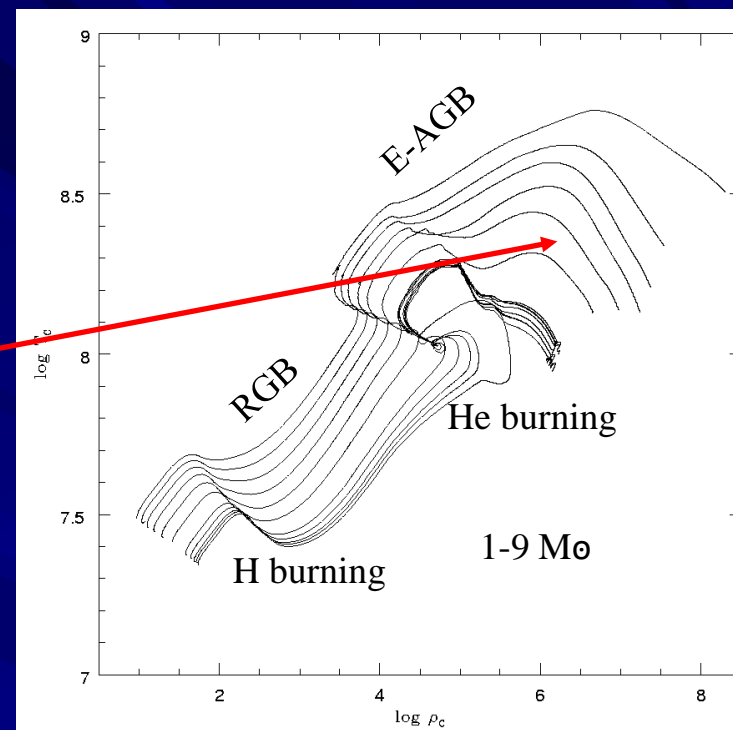
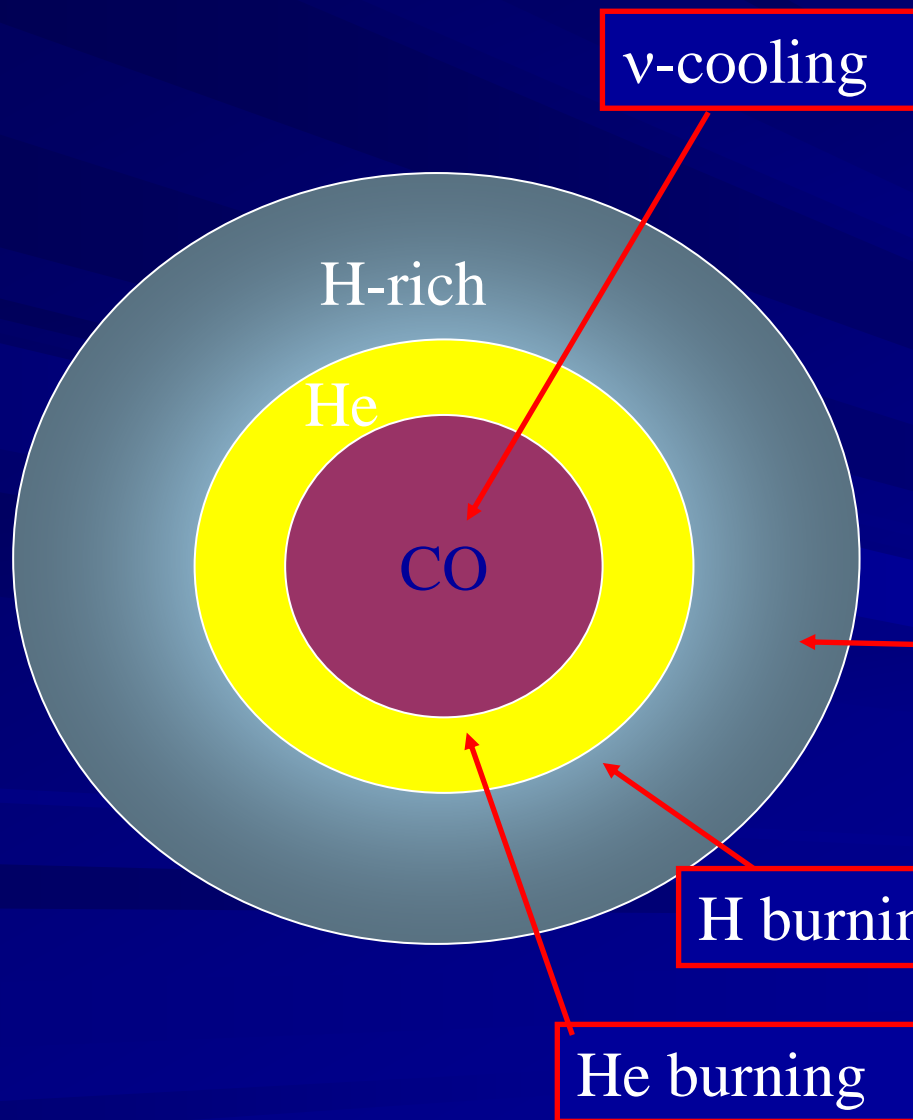


SiCs

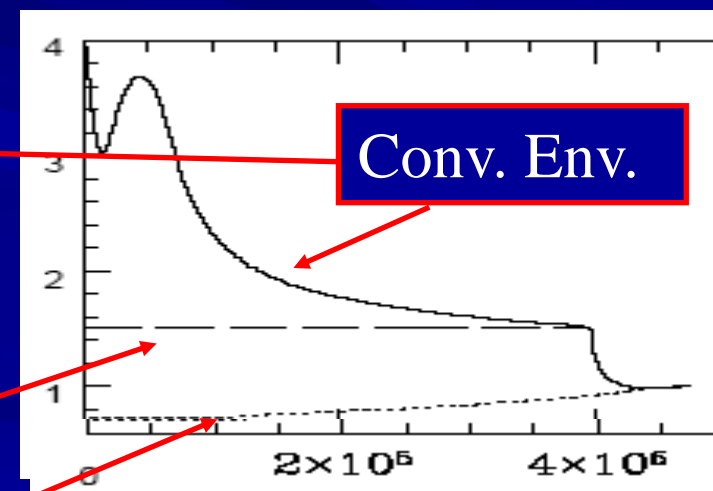


Graphites

Beyond the core He burning: the early-AGB

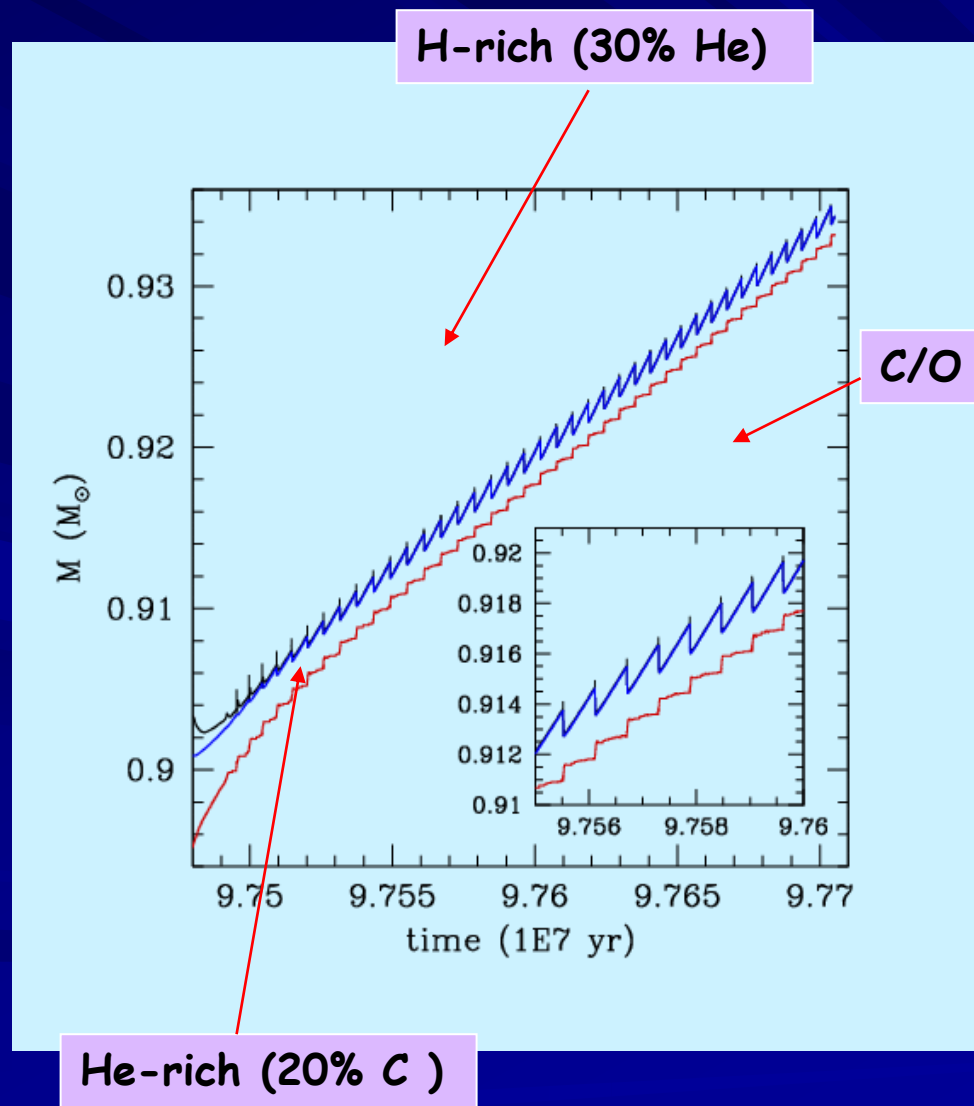
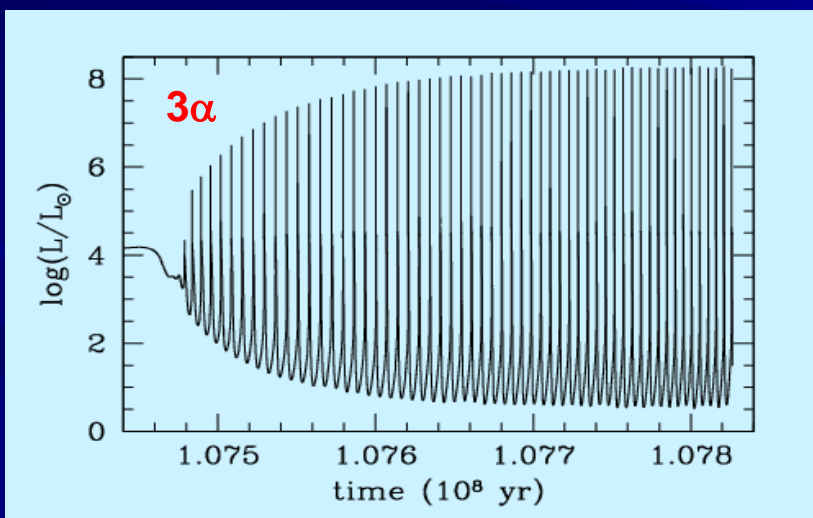
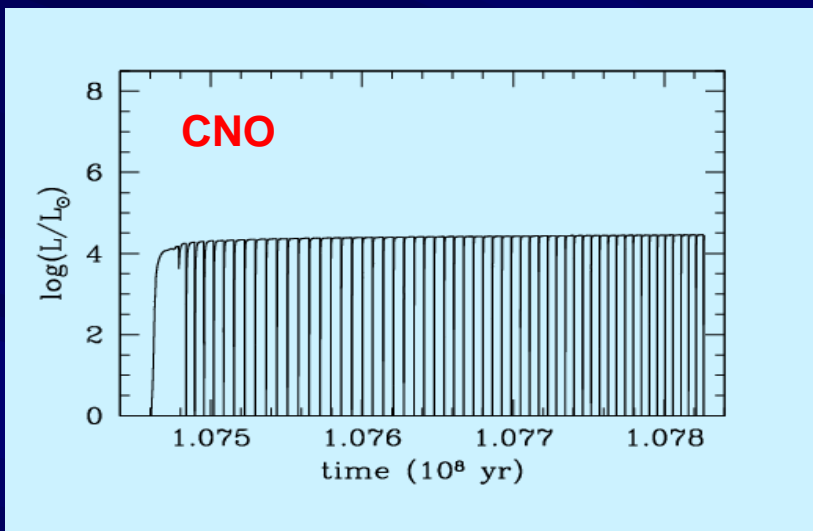


Central temperature vs central density for 1-9 M_{\odot} evolutionary tracks



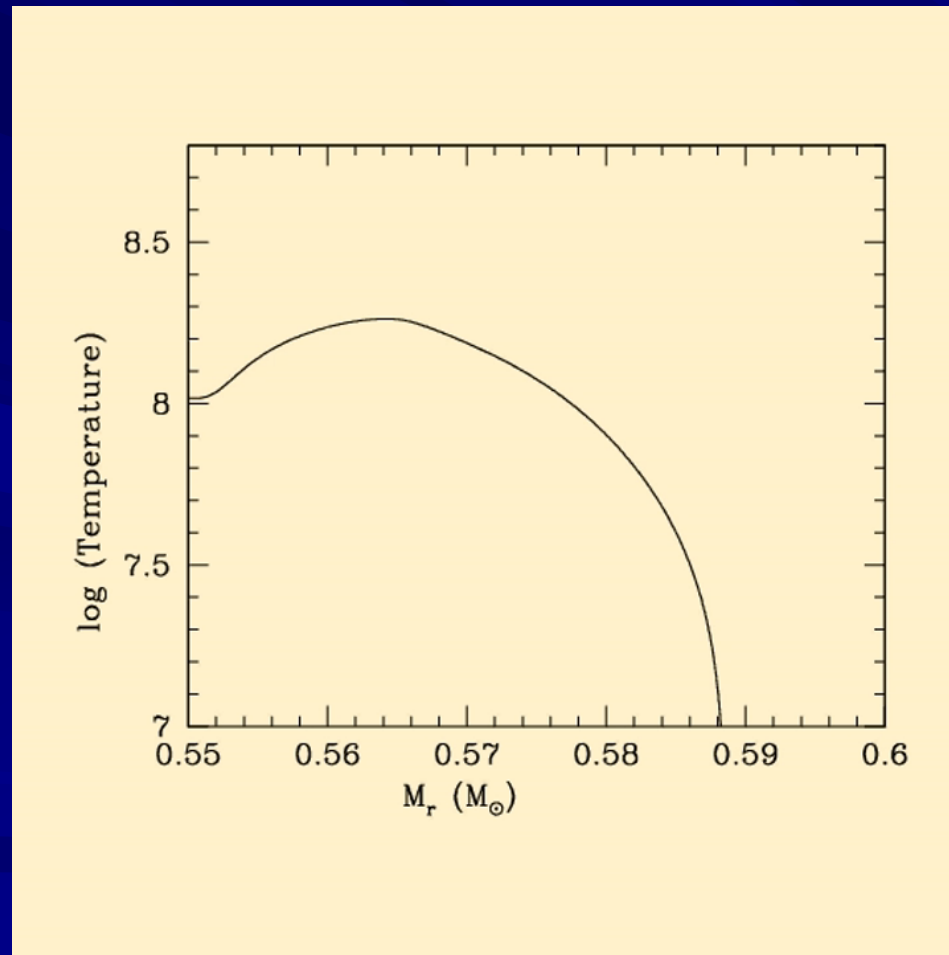
Second dredge up

Thermal pulses and TDU in AGB stars

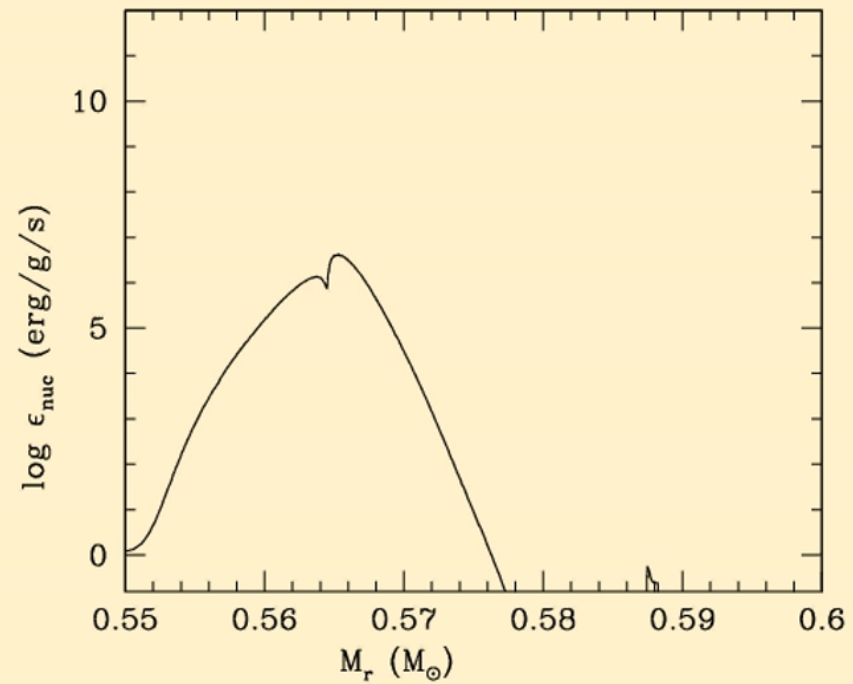


- For most of the time, the H-burning (upper panel) provides the energy to sustain the star shine.
- When enough helium has been accreted on top of the H-exhausted core, a He flash occurs (lower panel), eventually followed by a third dredge up (TDU).

The movie shows the evolution of the temperature profile in the intershell zone before and during a thermal pulse



The movie shows the evolution of the ϵ_{nuc} profile in the intershell zone before and during a thermal pulse



Questions about neutron-capture nucleosynthesis in AGB stars

- Since Merrill 1952, Tc is observed alive in these stars. It probes that neutron-capture processes are active. Which reactions can provide neutrons?

and related to that:

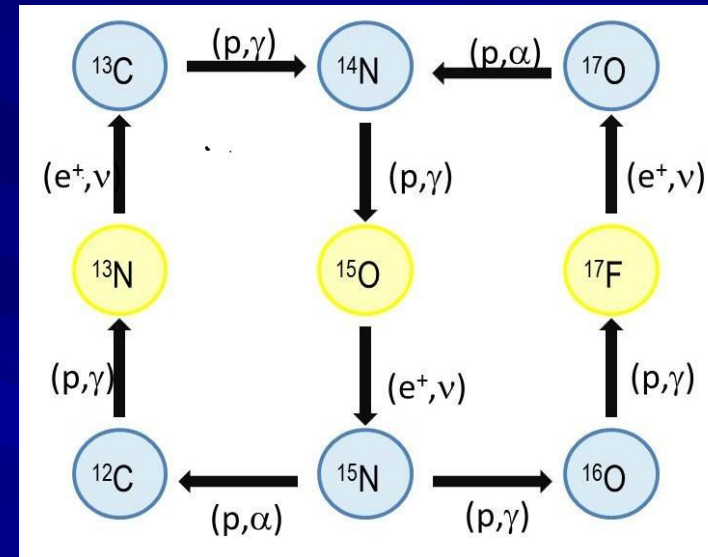
- What are the required neutron density and neutron exposure?

Abundance measurements in low-mass AGB stars and their daughters (post-AGB), tell us that the neutron density should be small ($\rho = 10^6$ - 10^7 neutrons/cm³), but the neutron exposure, i.e. $\tau = \int \rho v_{th} dt$ (where v_{th} is the thermal velocity) should be large (0.1-0.5 mb⁻¹).

The two burning shells

- H burning shell \rightarrow CNO cycle \rightarrow α and ^{14}N

..... also traces of ^{13}C



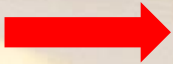
- He burning shell $\rightarrow 3\alpha$ and $^{12}\text{C} + \alpha \rightarrow ^{12}\text{C}$ and ^{16}O

..... also $^{14}\text{N}(\alpha,\gamma)^{18}\text{F} \rightarrow ^{18}\text{O}(\alpha,\gamma)^{22}\text{Ne}$

- Possible neutron sources $^{22}\text{Ne}(\alpha, n)^{25}\text{Mg}$ and $^{13}\text{C}(\alpha, n)^{16}\text{O}$.
- Before the 1990s, all the proposed scenarios for AGB s process nucleosynthesis supposed that the neutron source was active during the thermal pulse (see, e.g., Iben and Renzini 1984).
- It implies high temperature (300 MK or 30 keV), high neutron density (10^{11} - 10^{13} cm⁻³), but short timescale (months), so that the neutron exposure is quite (too) low.
- All these features are in contrast with the observed nucleosynthesis yields.

s-Process paradigm for low-mass AGB (1.2-3 M_{\odot})

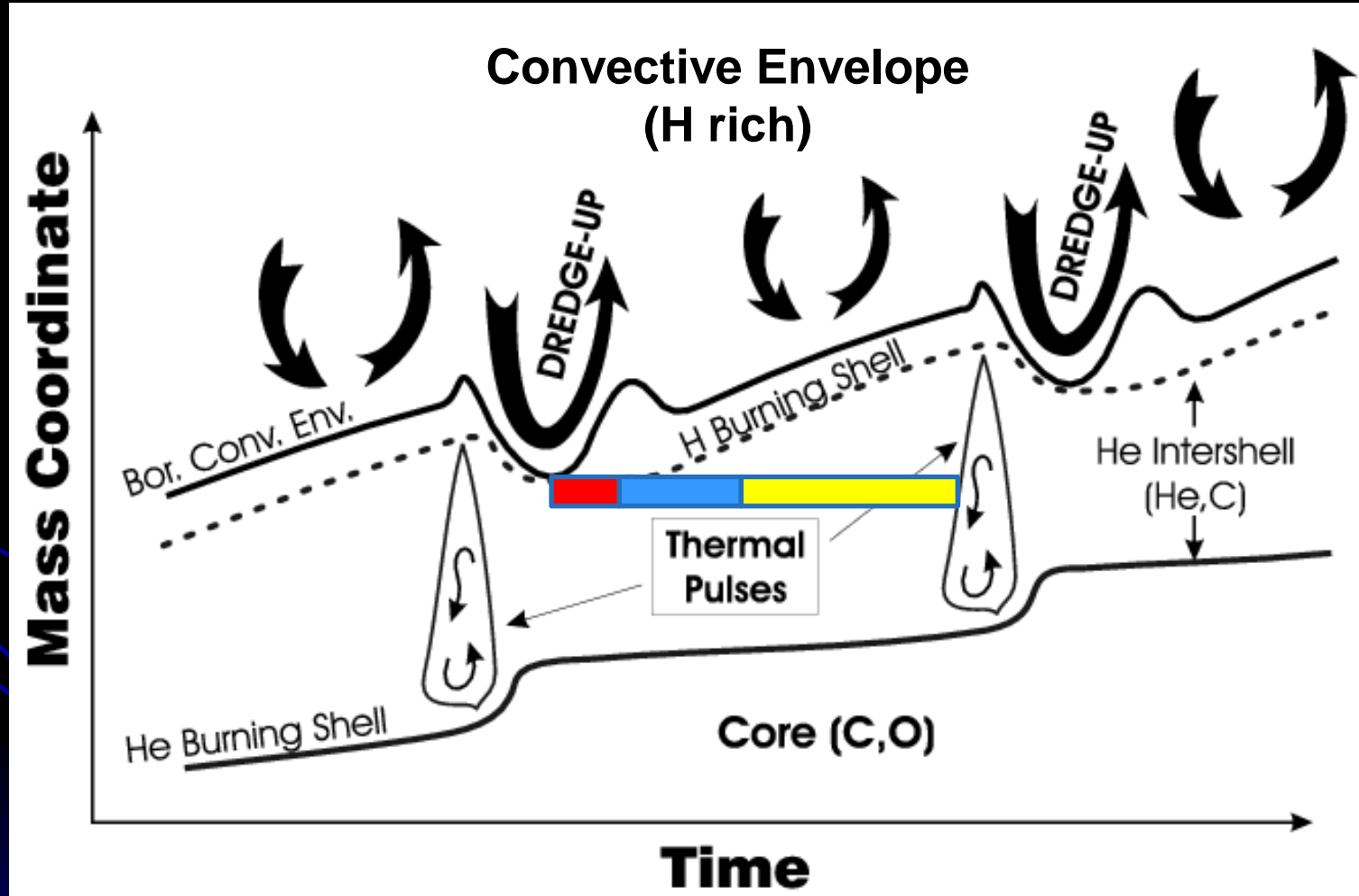
Straniero et al. 1995 - Gallino et al. 1998

Bagnasciuga (wet&dry) 

A ^{13}C pocket shall form in the transition strip between the sea (convective env.) and the shore (core)

s-Process paradigm for low-mass AGB (1.2-3 M_{\odot})

Straniero et al. 1995 - Gallino et al. 1998



**The «radiative ^{13}C -pocket scenario» has two specific features:
i) high neutron exposure and ii) low neutron density.**

Neutron exposure: $\tau = \int \rho v_T dt$

Typical numbers: $\rho=10^7 \text{ cm}^{-3}$, $v_T=8 \text{ KeV}$, $\Delta t=10^5 \text{ yr}$ and $\tau=0.4 \text{ mb}^{-1}$

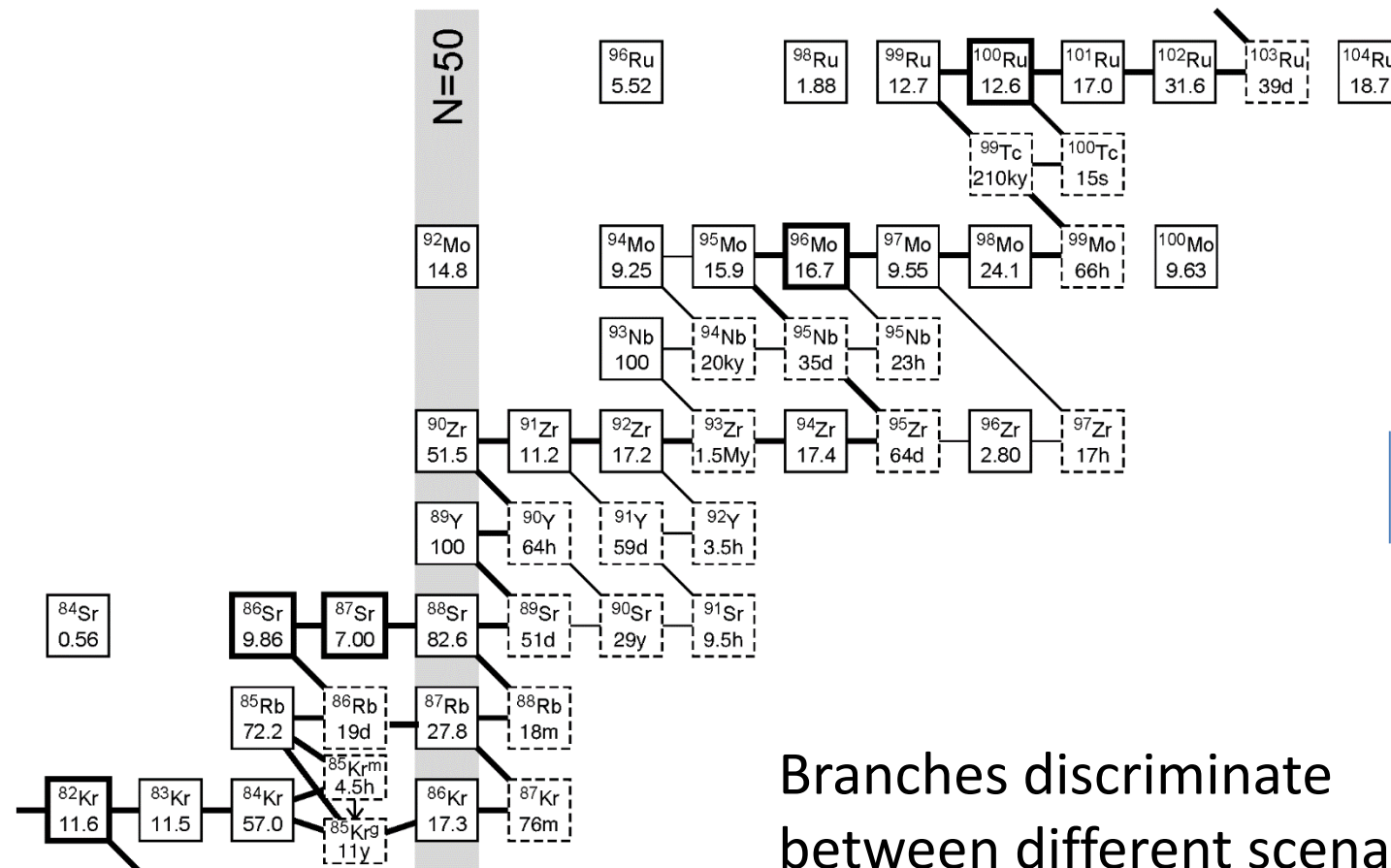
A neutron exposure of this order of magnitude allows the production of the s-process main component ($90 < A < 204$).

Such a low neutron density explain the isotopic and elemental abundance ratios nearby the critical branches of the s-process path.

* 1 barn= 10^{-24} cm^2

Many observational confirmations of the low-mass AGB scenario:

- Low Rb/Sr in S and C stars (Lambert 1995, Abia 2001)
- Low ^{96}Zr in S stars and SiC grains (Zinner 1995, Lugaro 2003)



Branches discriminate between different scenarios

THE CHEMICAL COMPOSITION OF RED GIANTS. IV. THE NEUTRON DENSITY AT THE *s*-PROCESS SITE

DAVID L. LAMBERT,¹ VERNE V. SMITH,¹ MAURIZIO BUSO,² ROBERTO GALLINO,³ AND OSCAR STRANIERO⁴

Received 1995 January 11; accepted 1995 March 8

ABSTRACT

Rubidium abundances are determined from the Rb I 7800 Å line via synthetic spectra for a sample of M, MS, and S giants. The Rb abundance increases with increasing *s*-process enrichment. A ratio Rb/Sr \simeq 0.05 is derived for the *s*-processed material from the He-burning shell. Thanks to the branch in the *s*-process path at ⁸⁵Kr the Rb/Sr ratio may be used to determine the neutron density at the time of *s*-processing. The derived ratio is consistent with predicted neutron densities for operation of the *s*-process during the interpulse intervals in low-mass asymptotic giant branch (AGB) stars but clearly inconsistent with much higher neutron densities predicted for the running of the *s*-process in the He-shell thermal pulses of intermediate mass AGB stars and probably also of low-mass AGB stars.

Zirconium isotopic abundances are determined from ZrO bandheads near 6925 Å via synthetic spectra for a sample of S stars. No evidence is found for the isotope ⁹⁶Zr whose synthesis is controlled by the branch in the *s*-process path at ⁹⁵Zr. This observation shows that the observed stars are not intermediate mass stars with massive ($M_C \gtrsim 1 M_\odot$) cores. The absence of ⁹⁶Zr sets an upper limit on the neutron density at the *s*-process site which is higher than and, therefore, consistent with the limit set by the Rb abundances in related stars.

Subject headings: nuclear reactions, nucleosynthesis, abundances — stars: abundances — stars: late-type

Pressure scale height

• Hydrostatic equilibrium: $\frac{dP}{dr} = -g\rho$ $g = \frac{GM}{r^2}$

• Equation of state: $P = \frac{\rho}{\mu m_H} KT$

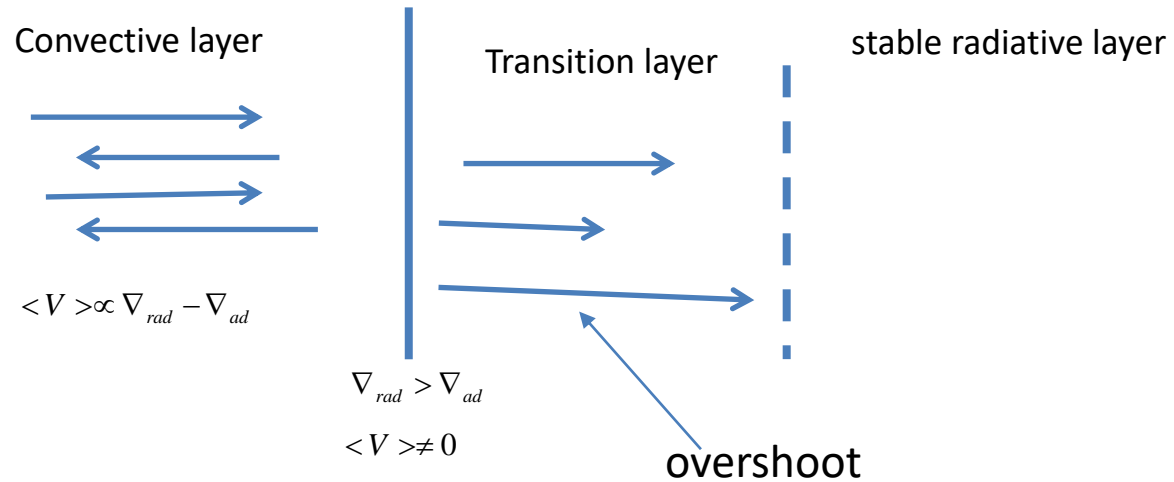
Combining: $\frac{dP}{P} = -\frac{\mu m_H}{KT} g dr = -\frac{dr}{H_P}$

where: $H_P = \frac{KT}{g\mu m_H}$ is the pressure scale height.

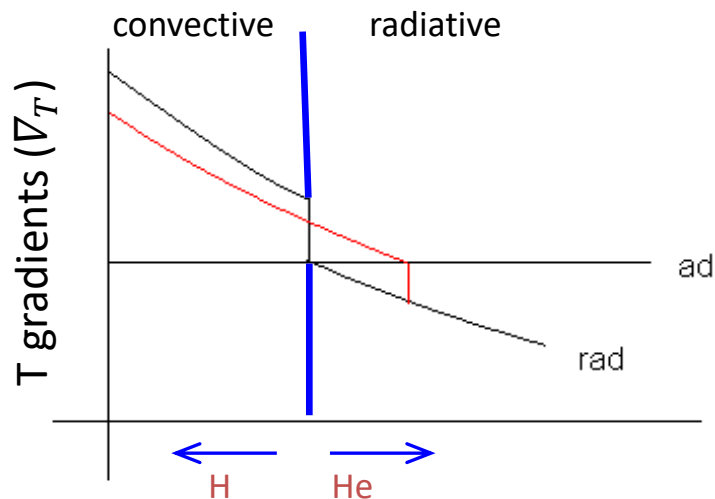
Then, on a small path (T, μ and g constants):

$$P = p_0 e^{-(r-r_0)/H_P}$$

Case b: dredge up



In case of dredge up, the H-rich envelope penetrates the He-rich mantel. The sharp variation of the chemical composition at the conv. border, causes a drop of the radiative opacity and, in turn, a sharp decrease of the radiative gradient. Then, the convective border becomes unstable and convection can easily penetrate inward. In this case, the overshoot induced by the chemical discontinuity is much larger



Hydrodynamical models of overshoot:

- 1) the penetration increases as the stability of the radiative layer below the convective zone decreases, e.g. Singh 1995
- 2) The velocity decays exponentially, e.g. Freytag 1996

Why an exponential decay of V?

Viscous dissipation of kinetic energy $\rightarrow \dot{r} = \dot{V} = -\alpha V^2$

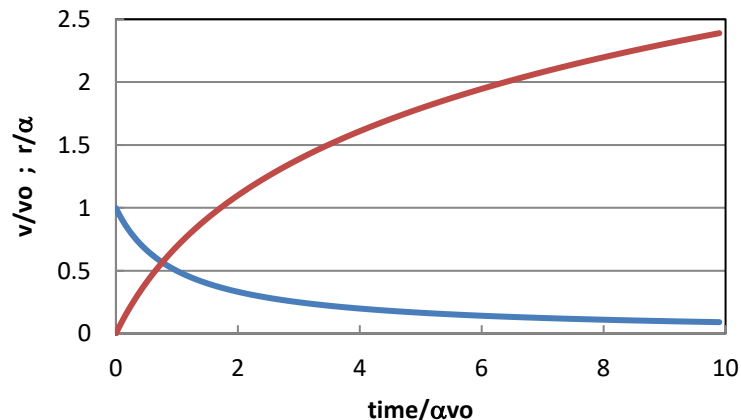
$$\frac{dV}{dt} = -\alpha V^2 \rightarrow \frac{dV}{V^2} = -\alpha dt \rightarrow \frac{1}{V} = \alpha t + \frac{1}{V_o}$$

$V[r(t)]$ = average velocity of a penetrating convective cell;

$V_o = V$ at the convective border ($r=r_o$ at time $t=0$)

$$V = \frac{dr}{dt} \quad \text{and} \quad W = \alpha V_o t + 1 \rightarrow dW = \alpha V_o dt$$

$$\frac{dr}{dt} = \frac{1}{\alpha} \frac{\alpha V_o}{\alpha V_o t + 1} \rightarrow dr = \frac{1}{\alpha} \frac{dW}{W} \rightarrow \delta r = r - r_o = \frac{1}{\alpha} \ln(\alpha V_o t + 1)$$

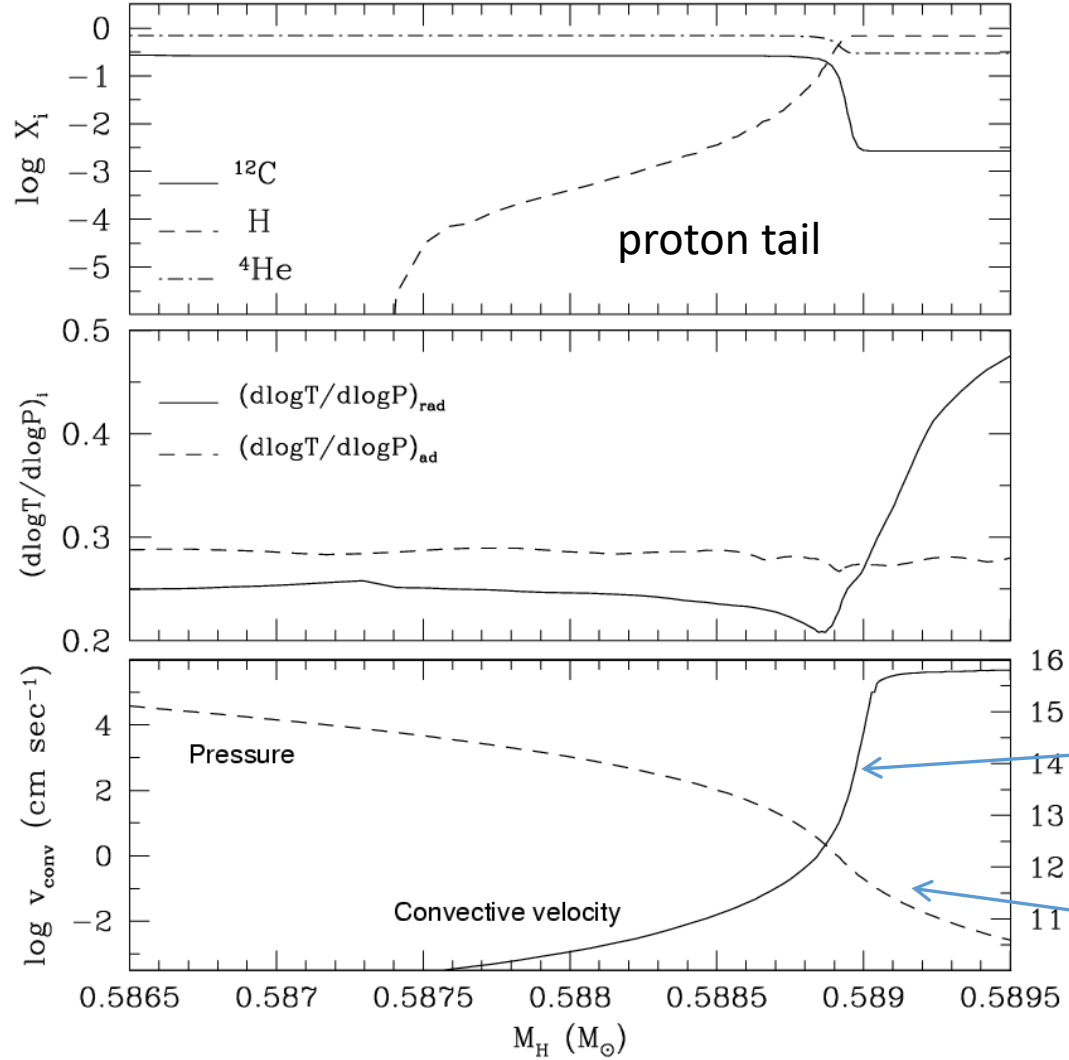


$$\alpha V_o t = \exp(\alpha \delta r) - 1 \rightarrow$$

$$V = V_o \exp(-\alpha \delta r)$$

$$\alpha = \frac{1}{\beta H_p}$$

Convective envelope attains the maximum penetration into the He core



Chemical stratification

Temperature gradient

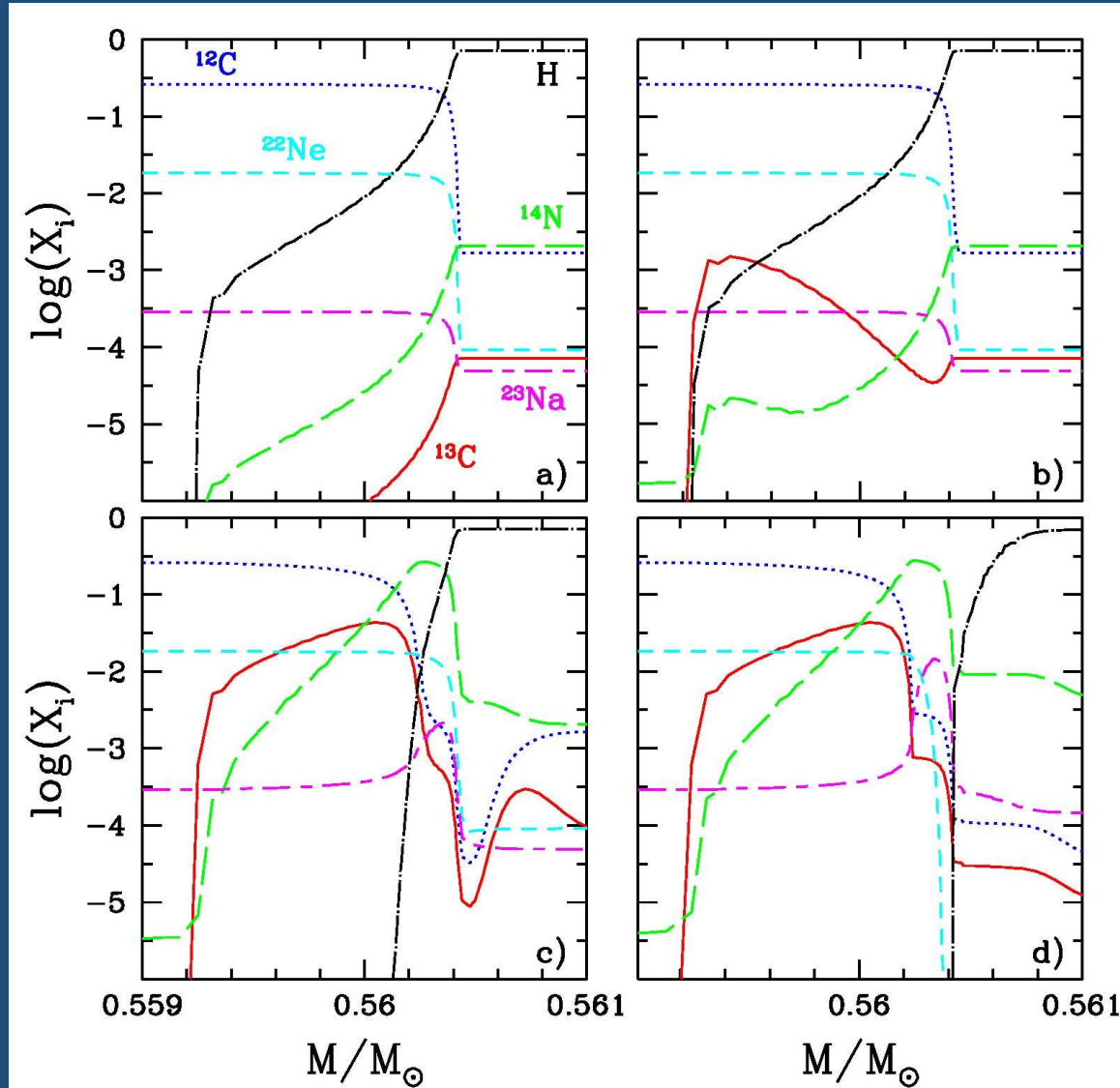
$$V = V_o \exp\left(-\frac{\delta r}{\beta H_p}\right)$$

$$P = P_o \exp\left(\frac{\delta r}{H_p}\right)$$



*note: below the convective envelope, $r < r_0$ or $\delta r < 0$

The formation of the ^{13}C pocket.



a)
Maximum envelope
penetration (TDU);

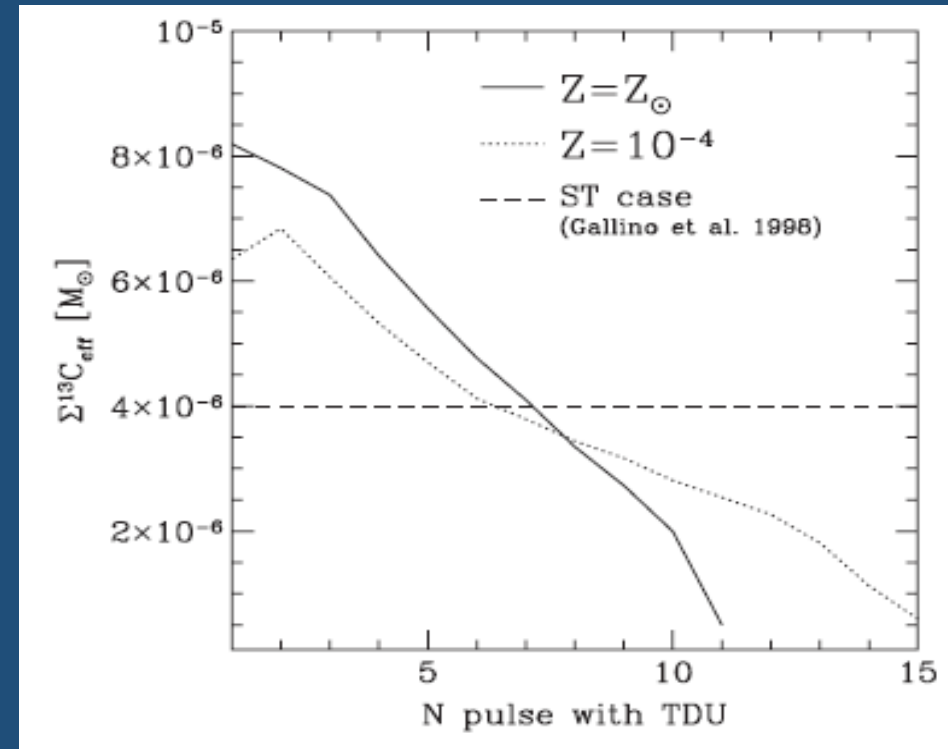
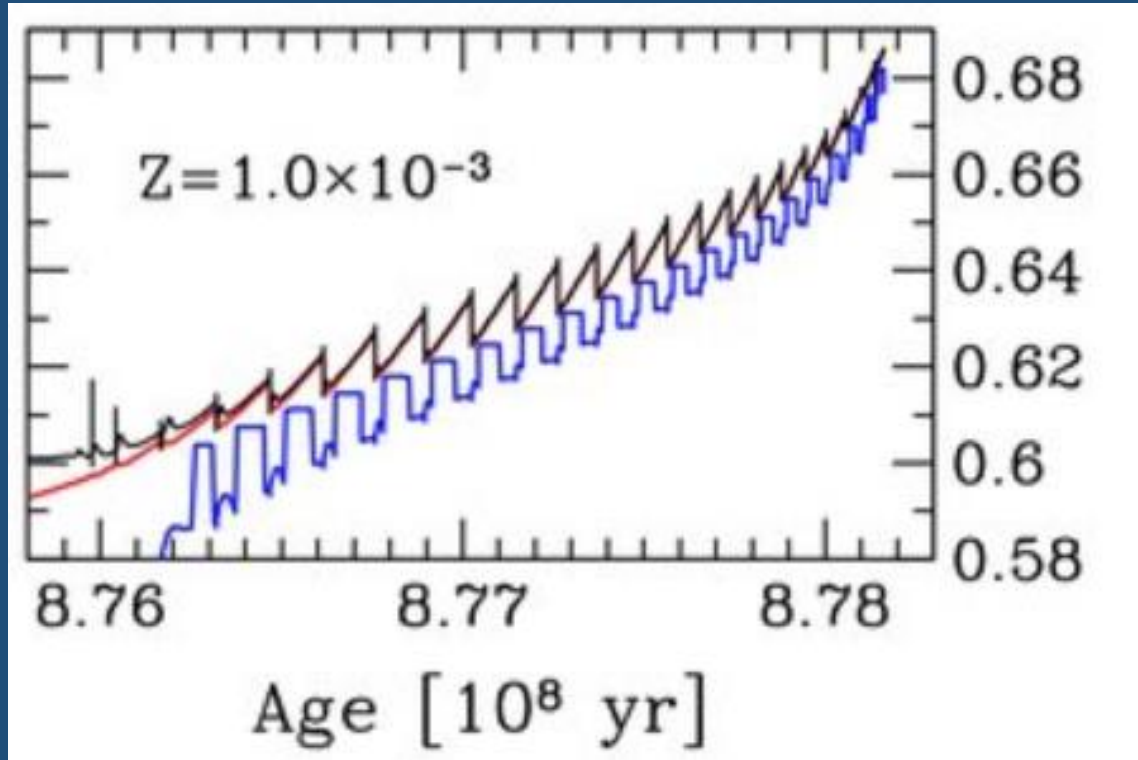
b) & c)
 $^{12}\text{C}(p,\gamma)^{13}\text{N}(\beta^-)^{13}\text{C}$
followed by
 $^{13}\text{C}(p,\gamma)^{14}\text{N}$;

d)
 $^{22}\text{Ne}(p,\gamma)^{23}\text{Na}$;

$$M=2M_\odot$$

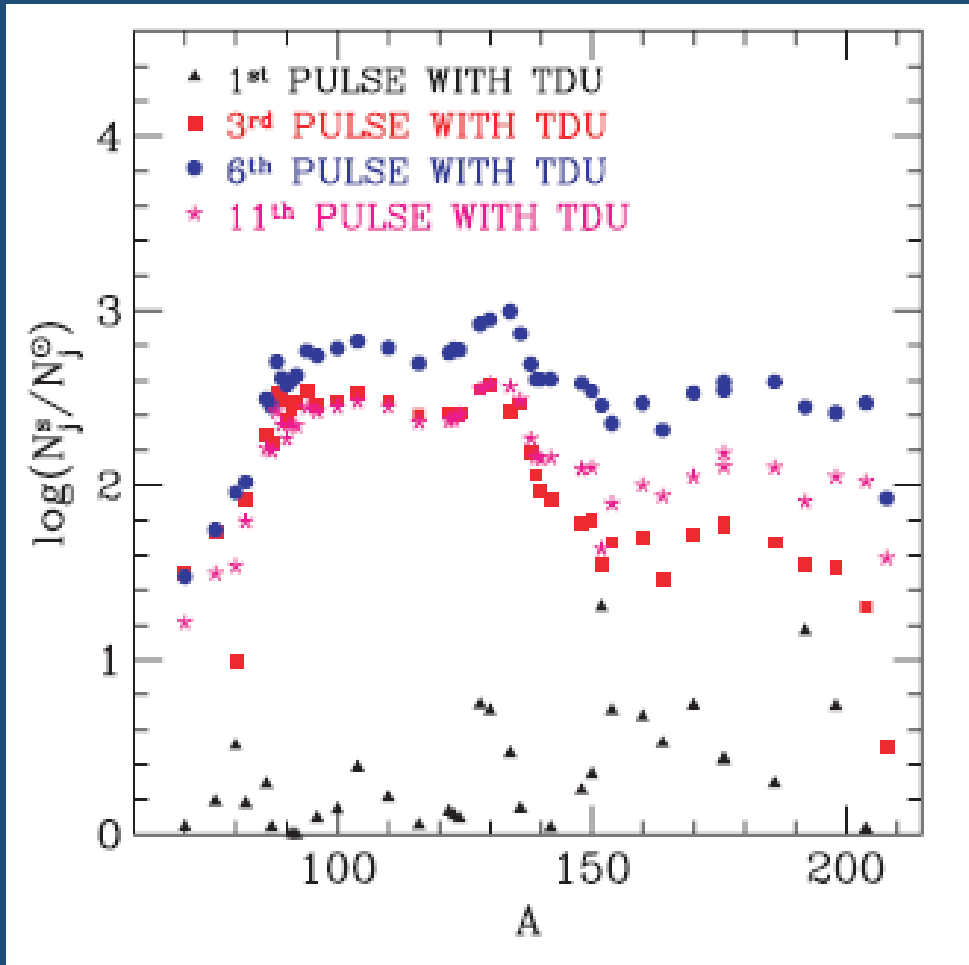
$$Z=Z_\odot$$

Nucleosynthesis in the He-rich mantel of AGB stars



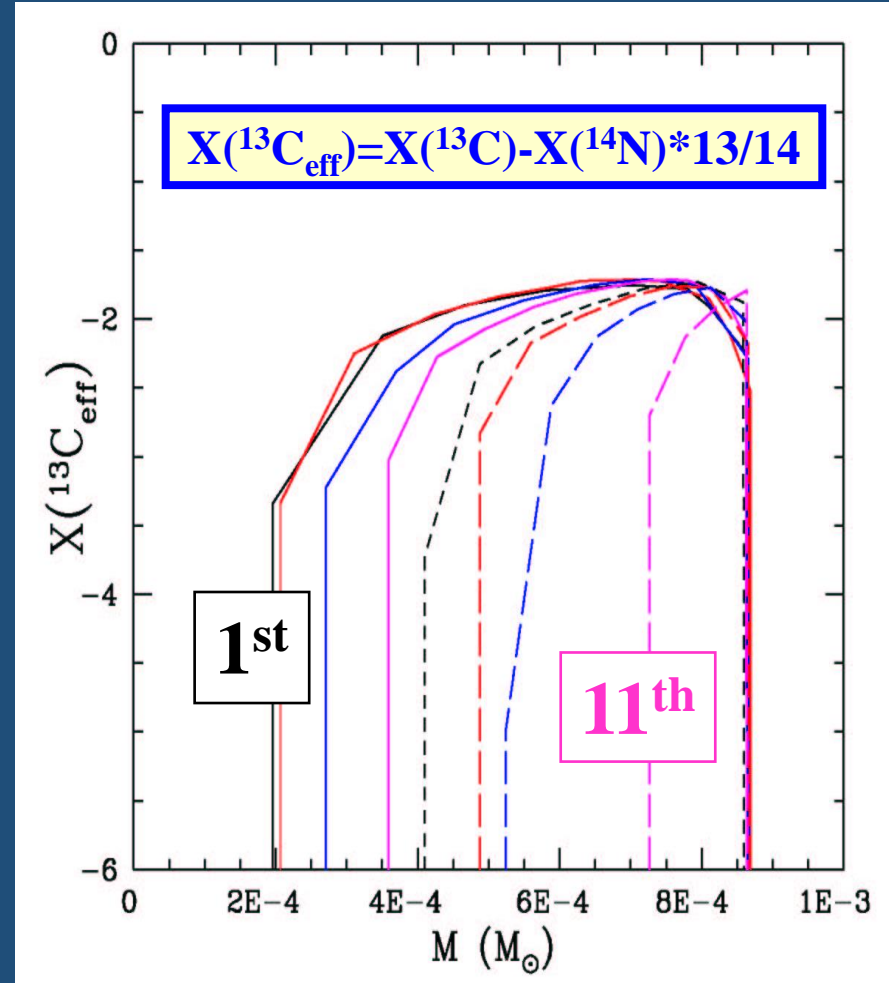
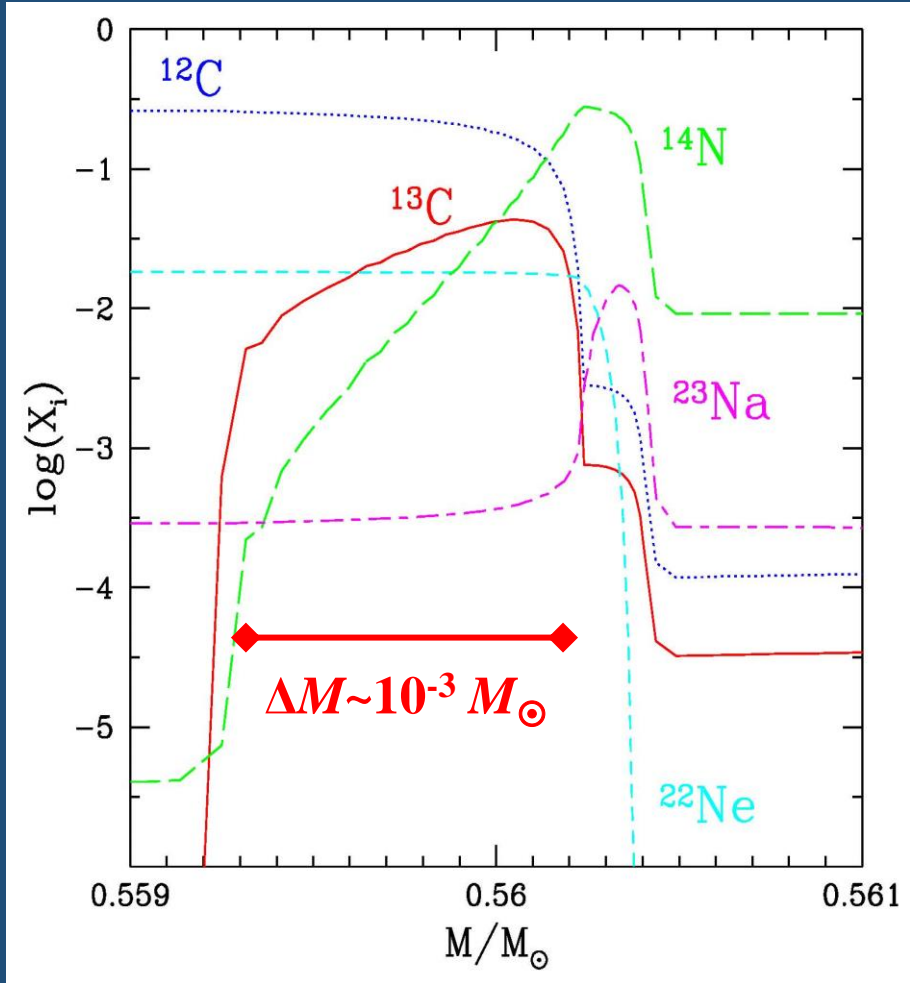
Multiple neutron exposures. After each TDU, a new ^{13}C pocket forms. Due to the overlap of the convective shells powered by the TPs, the final s-process yield is the cumulative contribution of all these pockets

Multiple neutron exposures in AGB stars



After each TDU, the ashes of the s-process are mixed and diluted with the envelope material. Heavy elements appear at the surface.

The resulting ^{13}C pockets



^{14}N strong neutron poison via $^{14}\text{N}(n,p)^{14}\text{C}$ reaction

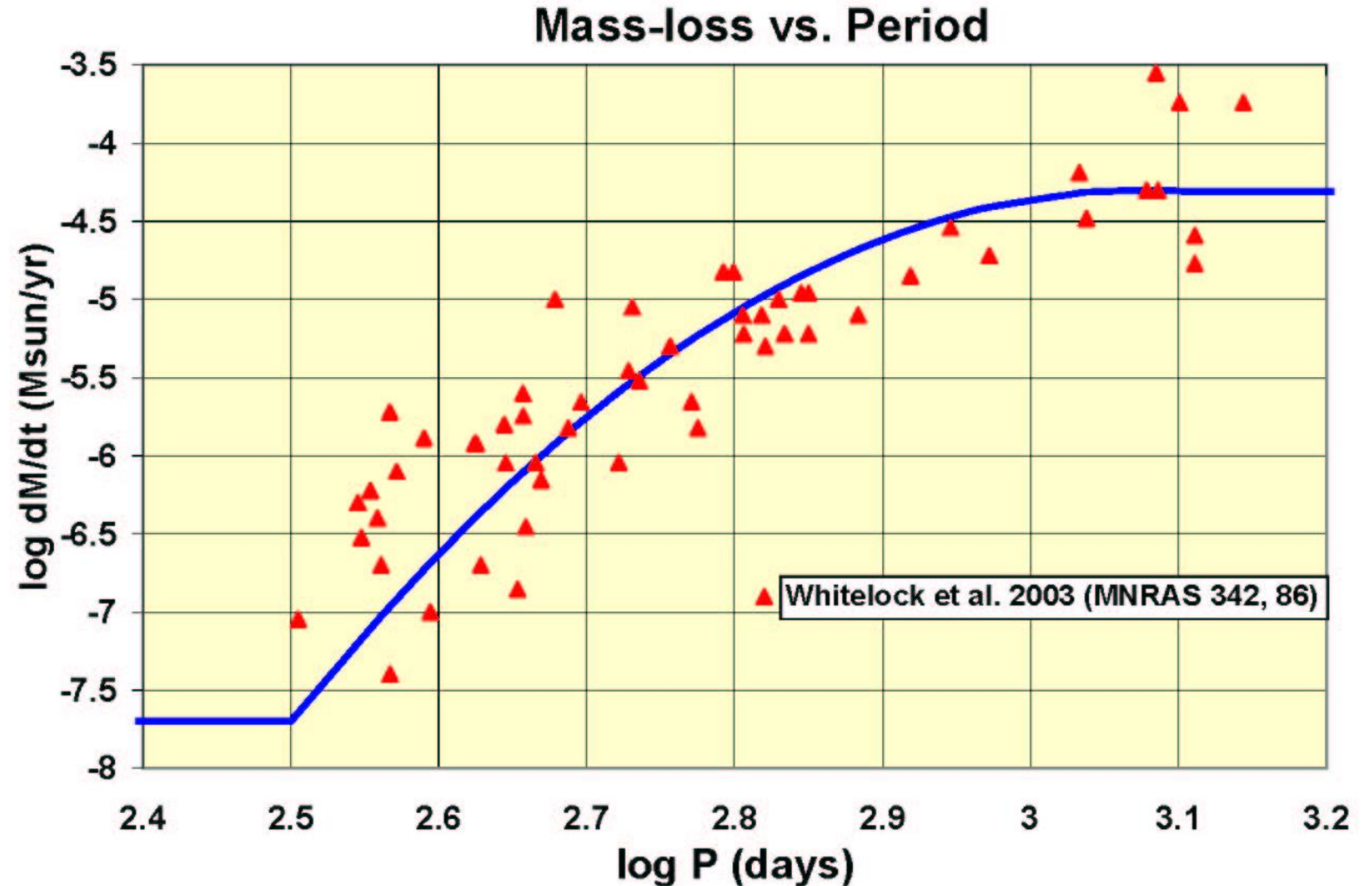
UP TO EARLY-AGB PHASE



REIMER'S MASS-LOSS
($\eta=0.2-0.4$)

*AGB MASS LOSS
is driven by
pulsation.*

*Stellar wind
determines the
duration of the
AGB and the
pollution of the
interstellar gas.*



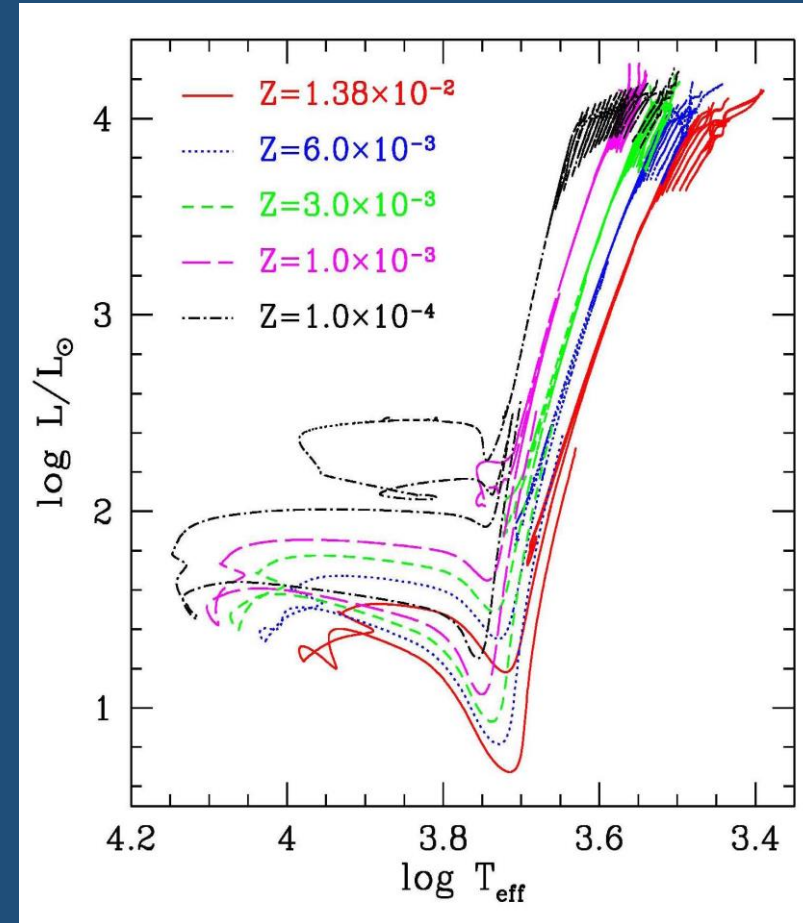
Results

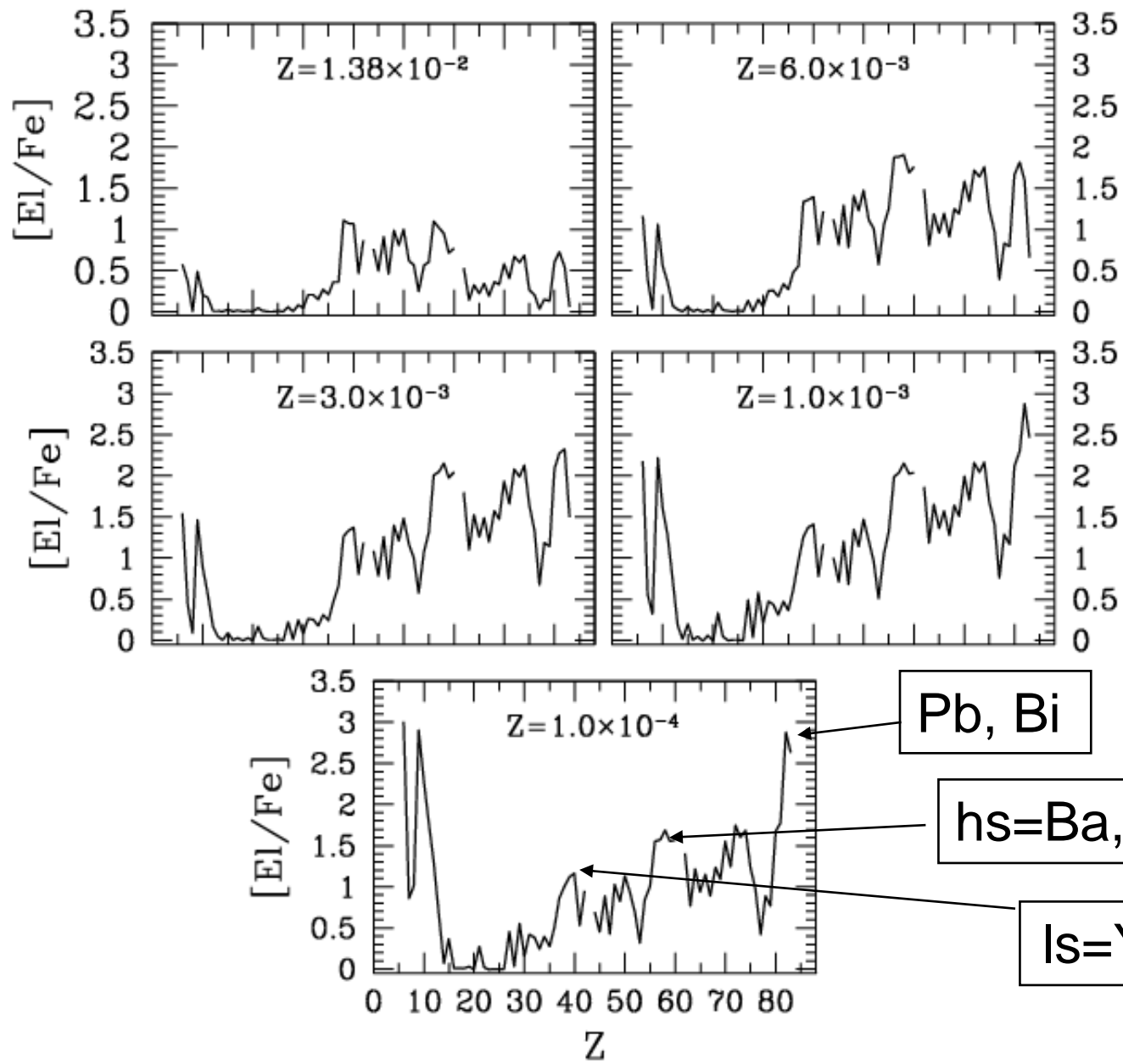
The C-rich opacities
make the stars redder in the
AGB phase.

When $C/O > 1$, new molecular species form,
such as CN, CH or C₂.



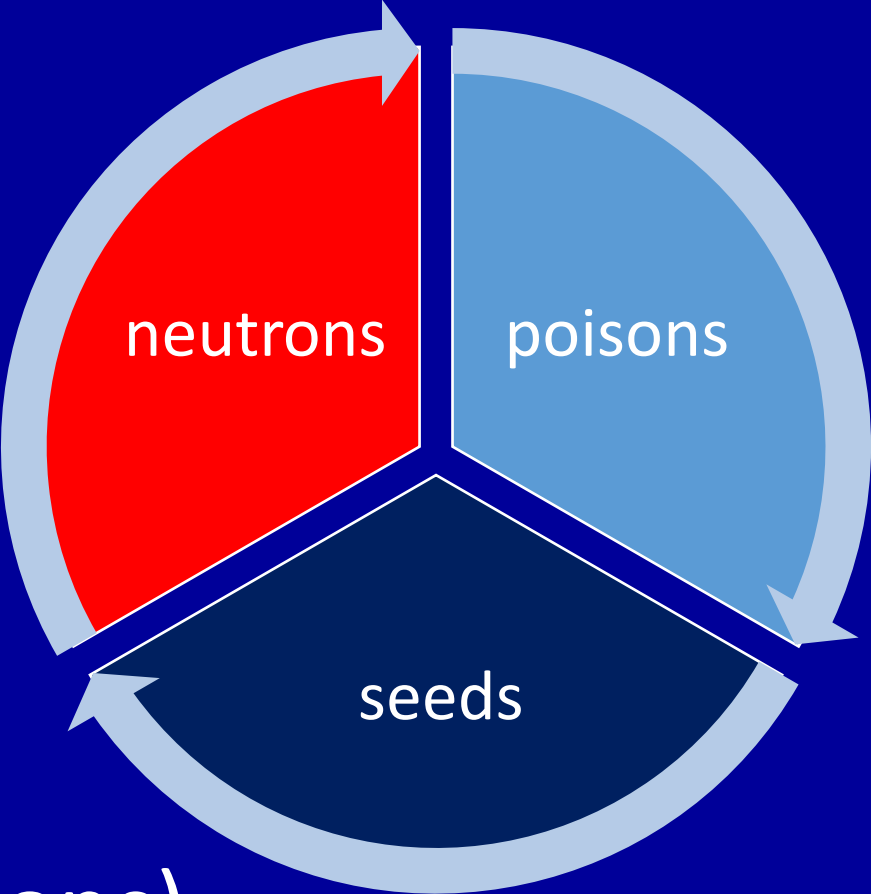
Affects integrated colors





Final AGB
composition for
 $0.0001 < Z < Z_{\odot}$

A 3 player game



(neutrons-poisons)
seeds



$$\begin{bmatrix} hs \\ \overline{\hspace{1cm}} \\ ls \end{bmatrix}$$

$$Y_n = \frac{N(\textit{neutrons})}{N(\textit{seeds})}$$

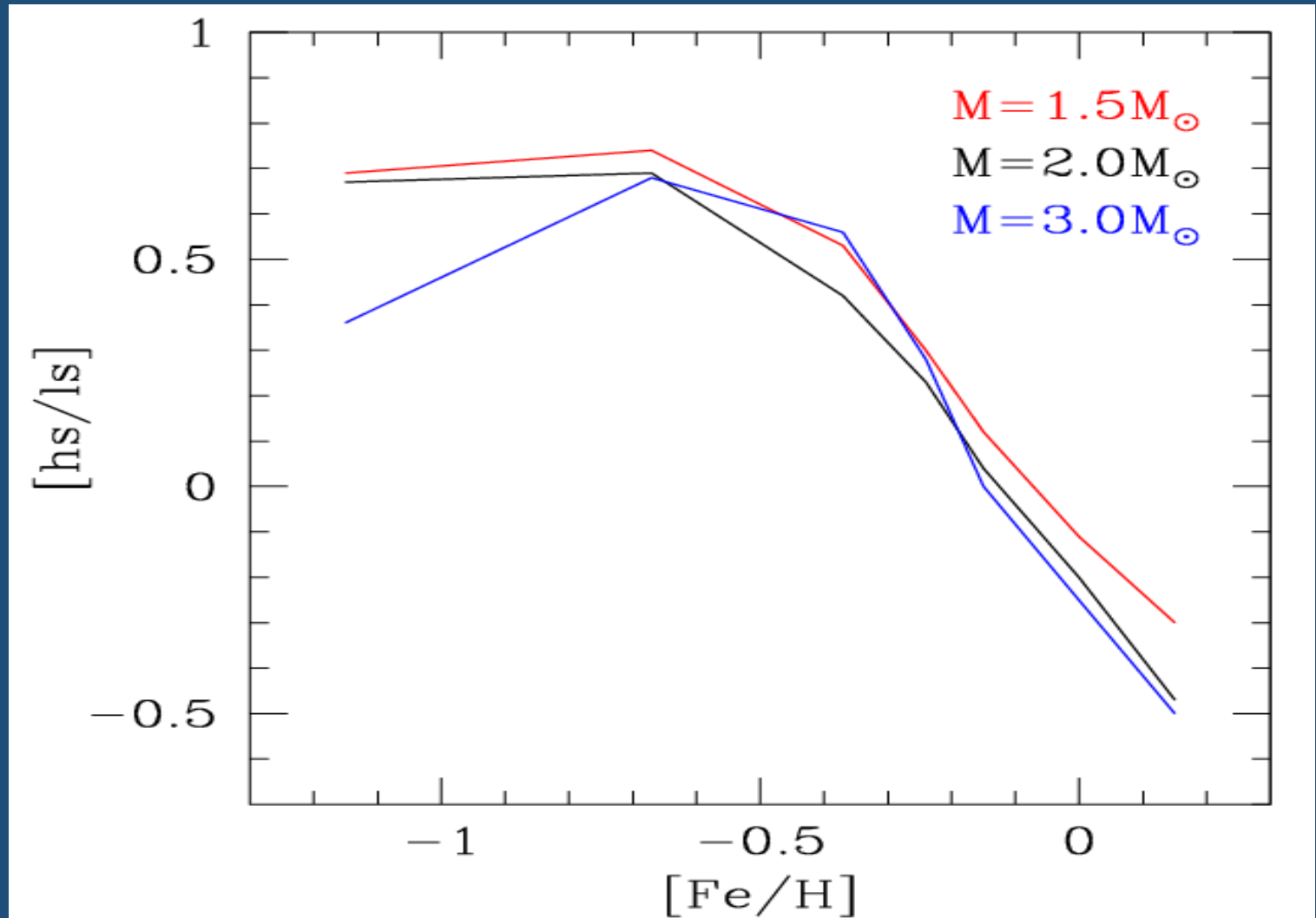
$$Y_n = \frac{N(^{13}\textit{C}) - N(\textit{poisons})}{N(^{56}\textit{Fe})} \approx \frac{N(^{13}\textit{C}) - N(^{14}\textit{N})}{N(^{56}\textit{Fe})}$$

Y_n decreases when the metallicity increases: more seeds (^{56}Fe) and more poisons (^{14}N), while the ^{13}C is more or less the same

$$\left[\frac{\text{heavy s}}{\text{light s}} \right] = \left[\frac{\text{Ba} + \text{La} + \text{Cs} + \text{Nd} + \text{Sm}}{\text{Sr} + \text{Y} + \text{Zr}} \right]$$

The larger the metallicity,
the higher the Y_n .

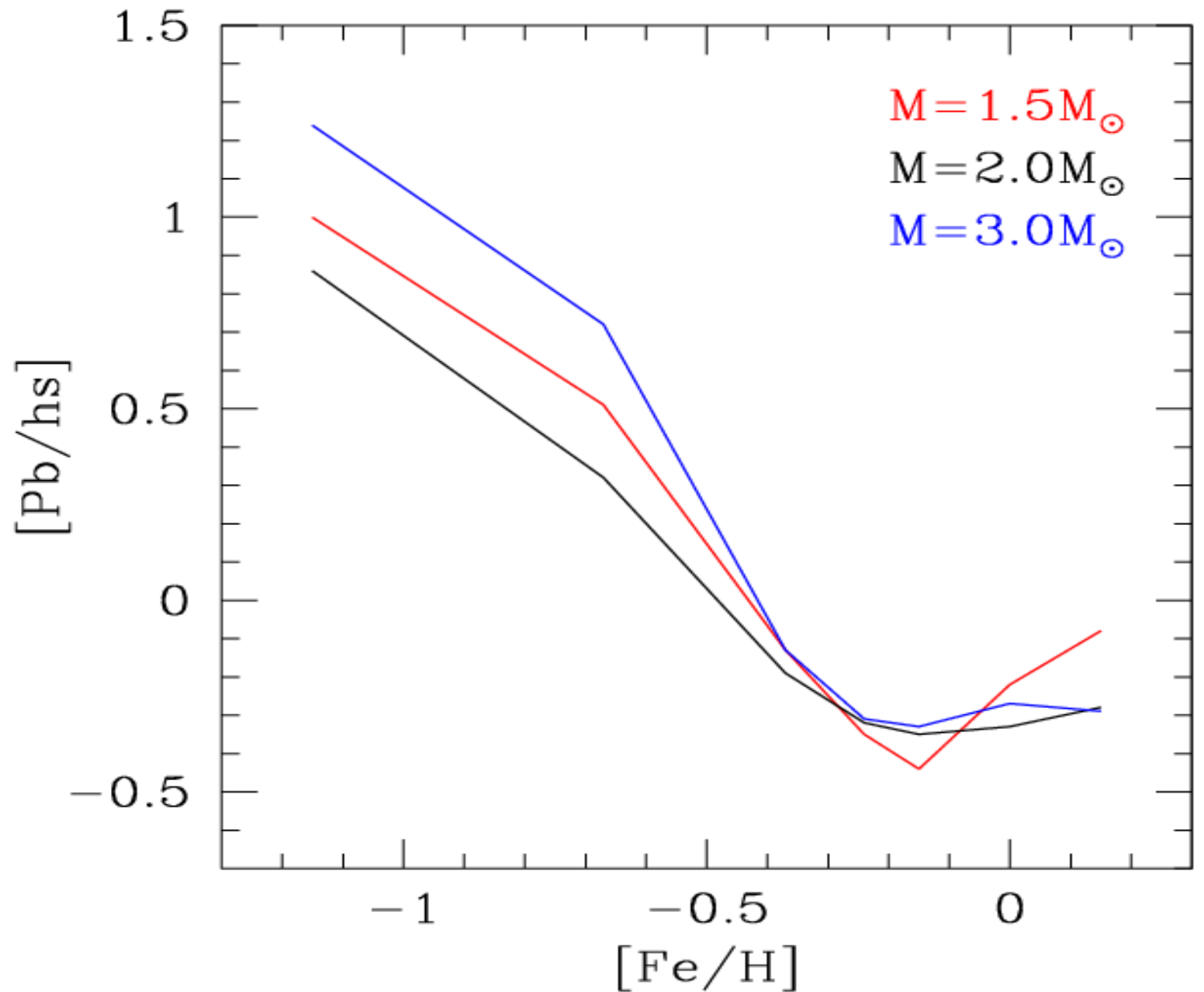
Ba, La, Cs, Nd and Sm
are produced at relatively
low Z , while *Sr, Y and Zr*
are the main products at
high Z



[Pb/hs]

Lead is produced by low-metallicity low-mass stars.

In these stars the neutron exposure may be larger than a few mb^{-1} .



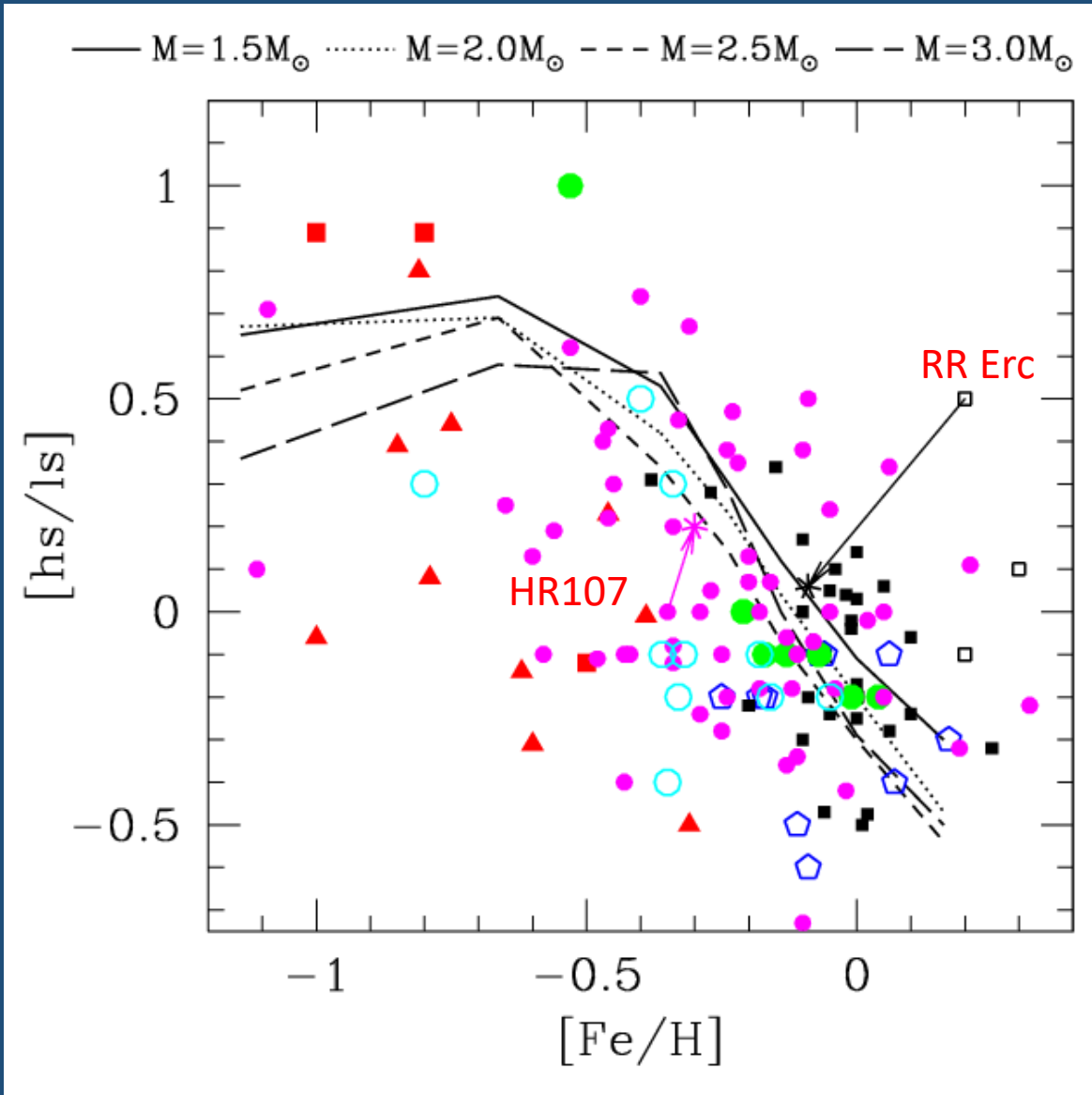
Varying the metallicity: theory versus observations

- ✓ **AGB stars undergoing TPs and III TDU** in the Galactic Disk or in nearby Galaxies (either O- and C-rich), like C(N type) stars. Tc detected (or low Nb).
- ✓ **Post-AGB stars showing s-process enhancements.**
- ✓ s-rich stars, dwarfs or giants (no Tc), like **Ba stars or CEMPs.**
- ✓ AGB imprints in pre-solar grains (**SIC or O-rich**).
- ✓ AGB imprints in the **Galactic Chemical Evolution.**

Model Constraints

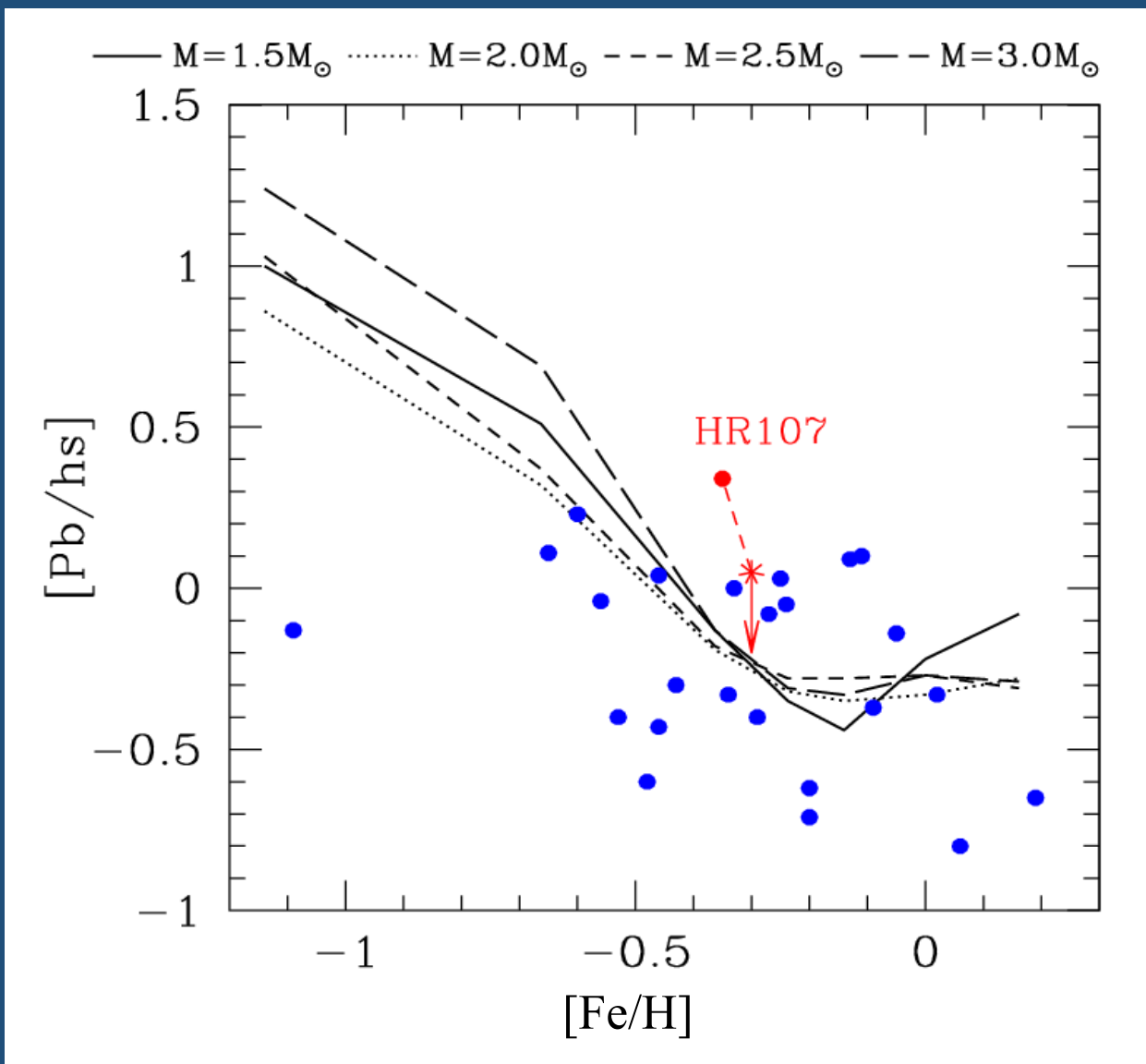
- **hs/ls:** is a measure of the neutrons/seeds ratio. It depends on the amount of neutrons (^{13}C), poisons (^{14}N) and seeds (Fe).
Better than X/Fe, which is affected by several uncertain quantities, such as mass-loss rate, dredge-up
- **Branching:** Rb/Sr or $^{96}\text{Zr}/^{90}\text{Zr}$. They depends on the neutron density and, in turn, on the temperature of the stellar site where they are syntesized....
- **AGB Luminosity Functions:** constraints for mass loss and dredge up efficiency.

Combining hs and ls



According to the standard paradigm, the [hs/ls] attains an asymptotic value after very few TPs (3 or 4). This index is independent on the evolutionary status of the observed star (Cristallo et al 2009).

Lead and hs



AGB nucleosynthesis is a complex interplay of several phenomena, among which convection and nuclear burning are the most important, but other physical processes may be in action.

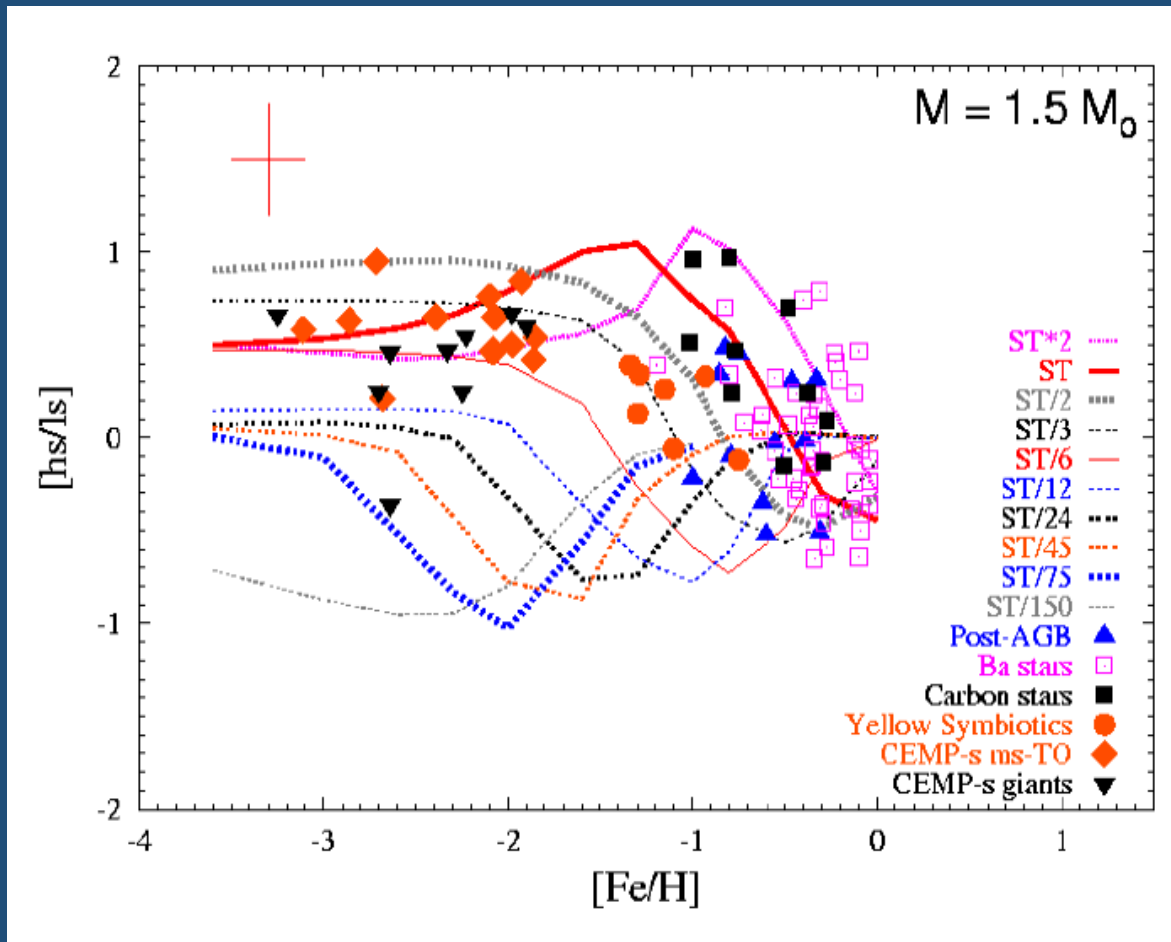
Interferences may be constructive or destructive, so that the resulting nucleosynthesis may be enhanced or suppressed.

Evidences for a more complex world:

- Spread of hs/l_s at different metallicity
- s-exceptions: **CEMPs and Ba-stars**

They are binary stars; in this case we see the secondary component of the binary, polluted with the material lost by the primary when it was on the AGB (see Bisterzo et al. 2011-2012). Today's the primary is a faint white dwarf

The Roberto Gallino recipe to explain the spread: star-to-star variation of the ^{13}C amount



The formation of the ^{13}C pocket is a stochastic process. In this case, a spread of the pocket size is naturally expected, so that stars with similar characteristics (mass, metallicity) may show different s-process enhancements.

Alternative n. 2: Poisons variation

- The same effect on (n-p)/seed may be obtained by varying the amount of poisons (like ^{14}N), instead of the ^{13}C .
- It is equivalent to reduce the *effective* ^{13}C
- An interesting case is obtained by considering mixings induced by stellar rotations.
- Rotation may induce several types of dynamical and secular instabilities.

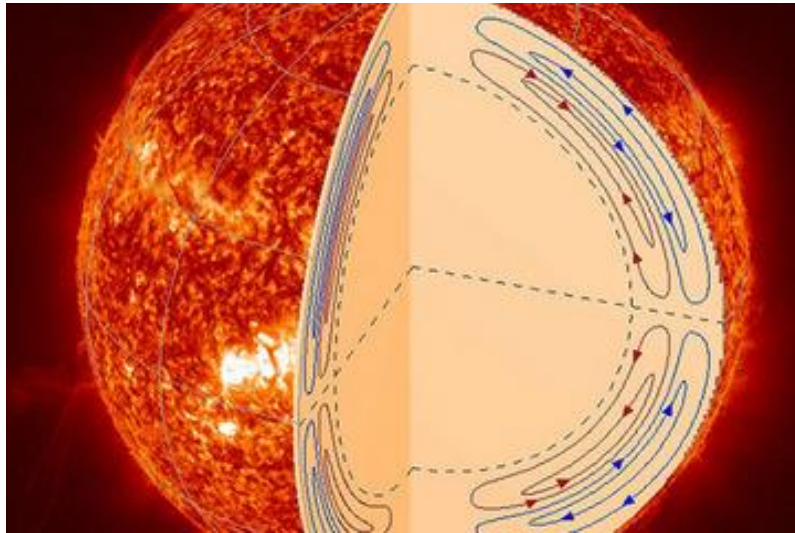
$$^{13}\text{C}_{\text{eff}} = ^{13}\text{C} - ^{14}\text{N}$$

In the He-rich zone of an AGB stars, in particular, Eddington-Sweet and shear instabilities are at work.

Additional processes....

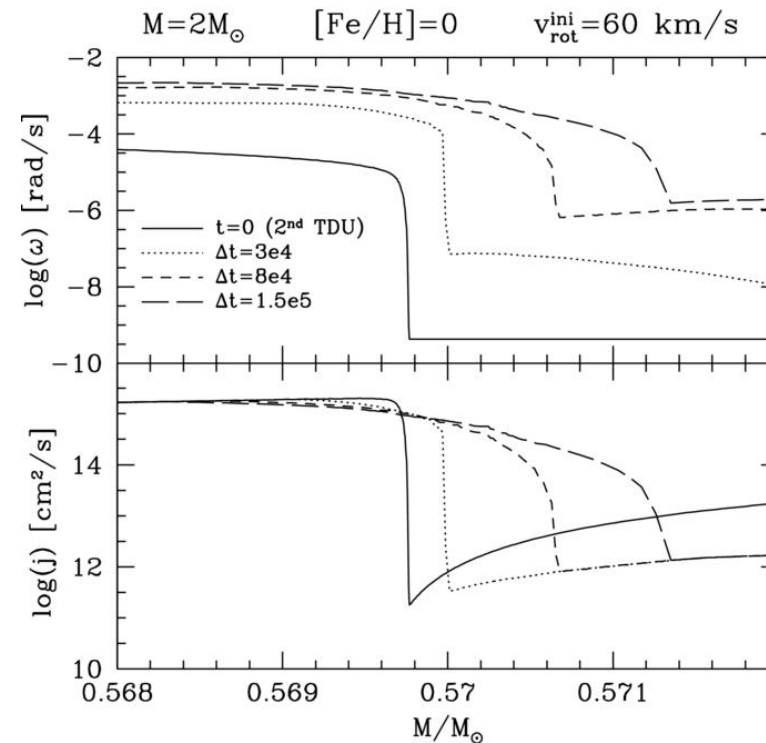
- Instabilities induced by **Rotation** may modify the H profile left by the third dredge up and, later on, the ^{13}C and the ^{14}N profile into the pocket (Piersanti et al. 2013).
- The bulk motion in the convective envelope generates **gravity waves** propagating inward. Turbulence may be generated by non-linear effects (Denussenkov 2003) or by interaction with rotation (Talon 2007). The consequent mixing may affect nucleosynthesis and angular momentum transport
- **Magnetic field** dissipates angular momentum (magnetic braking, Sujis 2008), but may also induce magnetic buoyancy, possibly operating in the He-rich intershell (see Vescovi et al. 2021).

Differential Rotation: ES + GSF instabilities during the interpulse



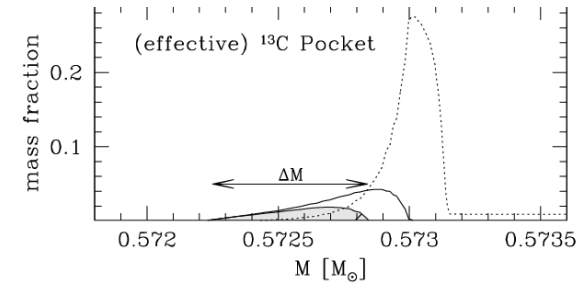
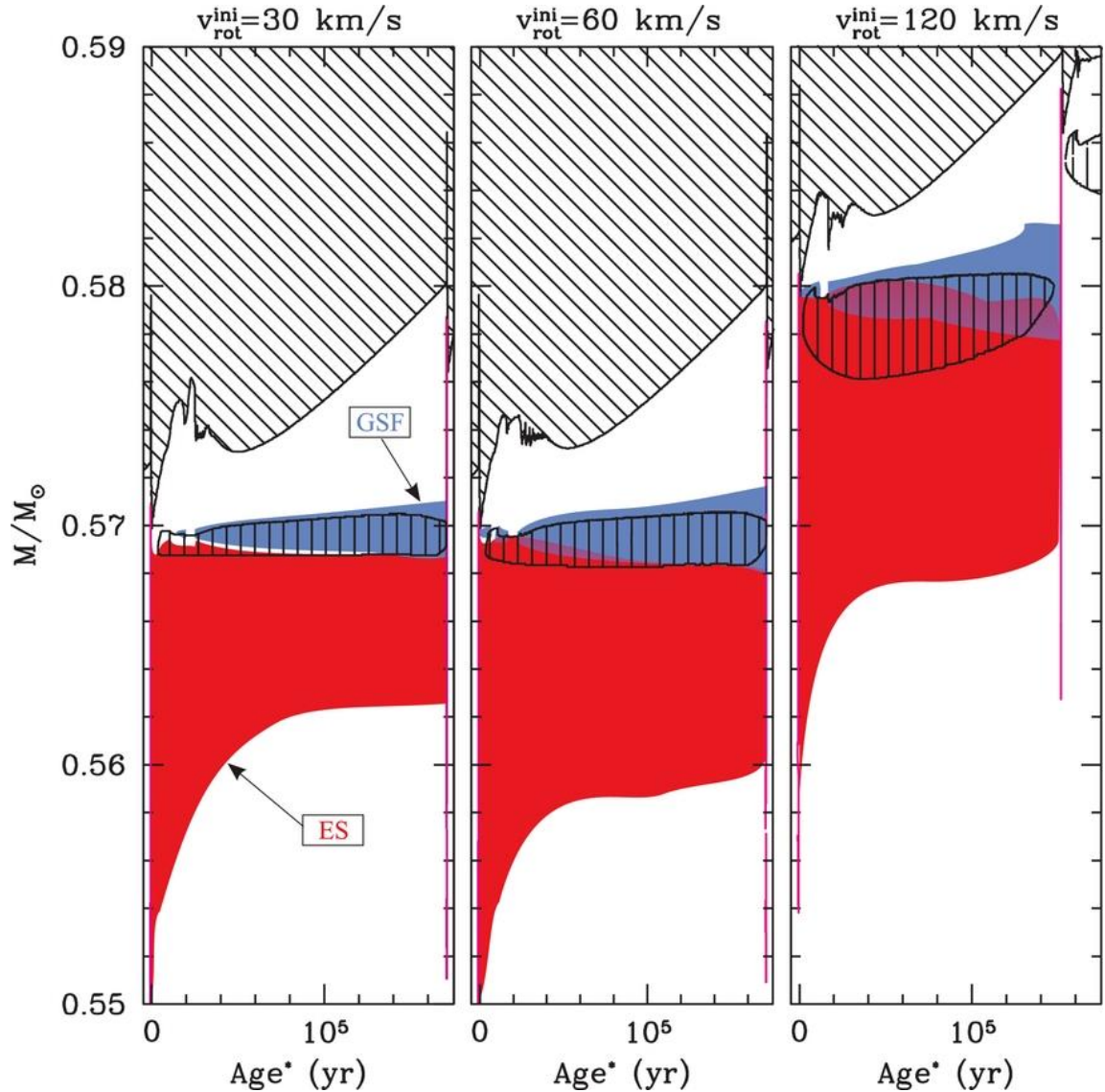
Meridional Circulation is always active in rotating stars, because of the von Zeipel effect, but it is inhibited by a μ gradient.

Sharp variations of ω and j left by the TDU drives GSF



See, e.g. Langer et al. 1999, Siess et al. 2004, Herwig et al. 2003, Piersanti et al. 2013

Development of rotation-induced instabilities between the 2nd and the 3rd TDU ($M=2 M_{\odot}$ $[\text{Fe}/\text{H}]=0$)



\\ convection

||| $X(^{13}\text{C}) > 10^{-3}$

■ ES

■ GSF

The rotation paradigm



+



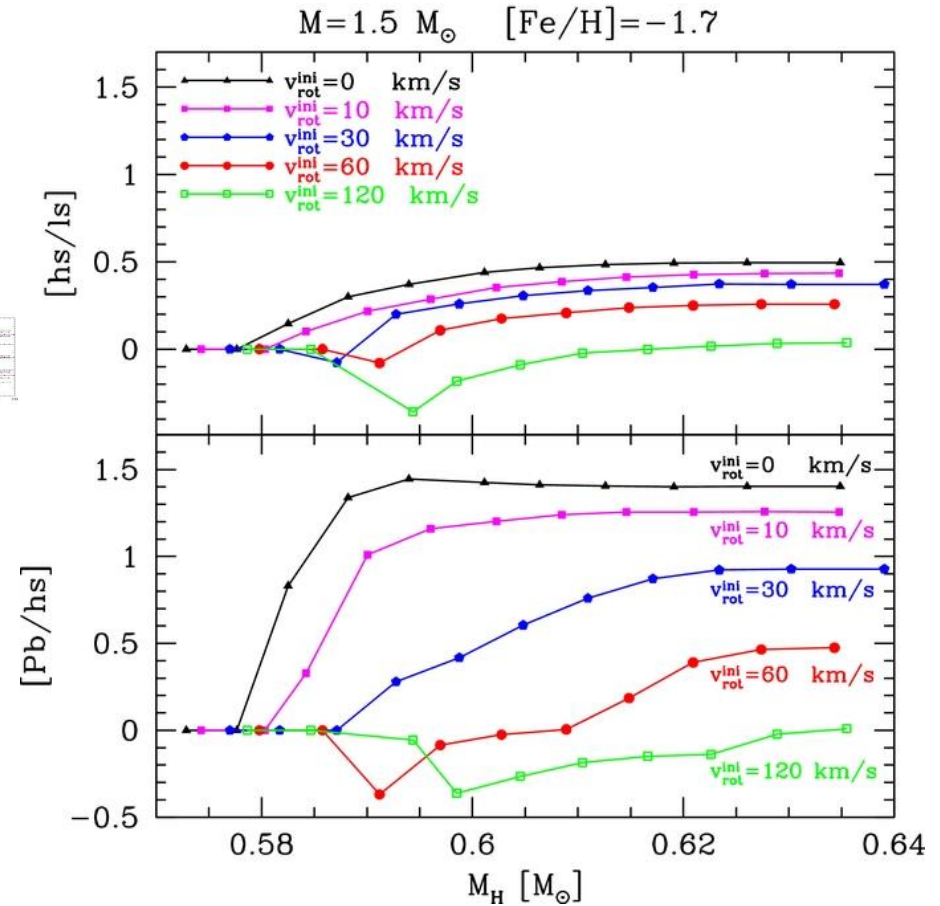
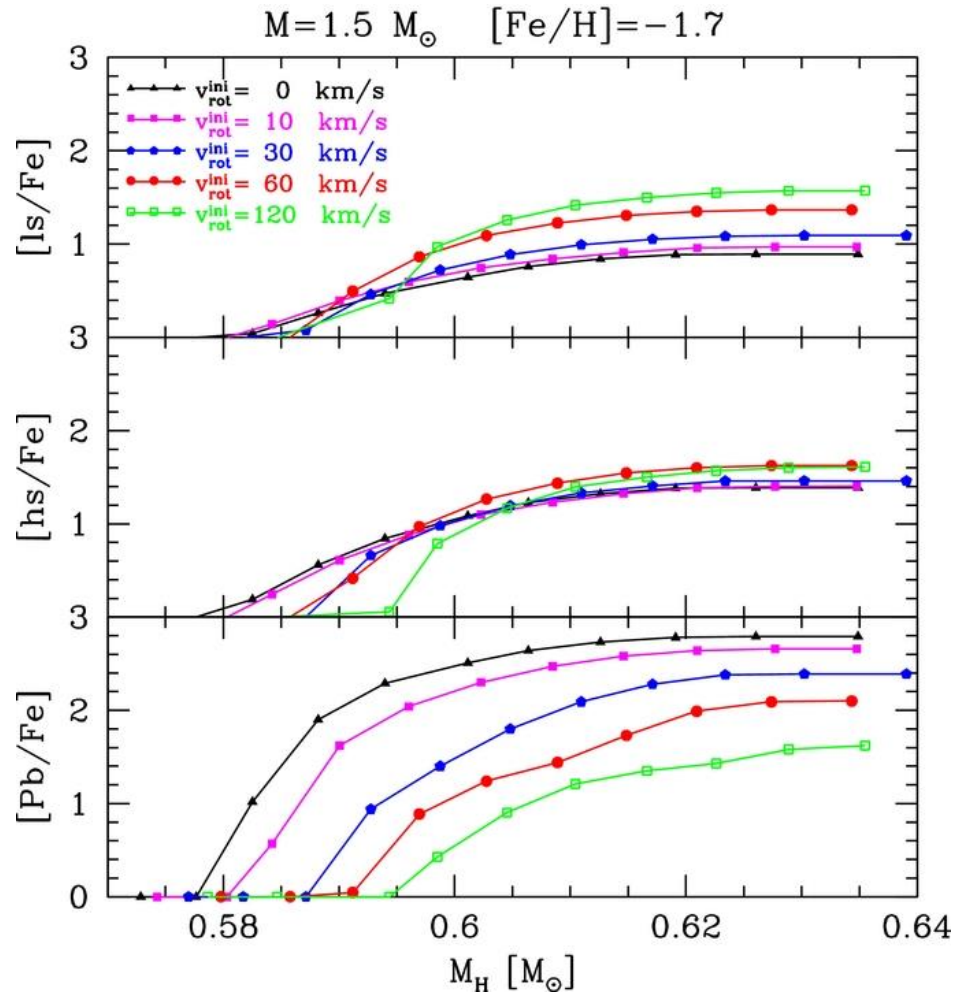
**Turbulent convection at TDU:
a proton profile forms at the top
of the He-rich zone**

**Rotation induced instabilities
during the interpulse: redistribution of
protons and, later on, of ^{13}C - ^{14}N
on a larger area. **Same neutrons, more
seeds and more poisons****

AS a result: lower $\frac{\textit{neutrons} - \textit{poisons}}{\textit{seeds}}$

Consequences of rotational induced mixing

From Piersanti et al. 2013



Summary of the rotation effects (Piersanti et al. 2013)

- Mixing induced by rotation may produce a partial or total overlap of the ^{14}N and ^{13}C pockets, so that the effective ^{13}C is reduced.
- Such an effect is expected to increase with the mass of the stars and with the initial V_{rot} .
- It may naturally imply a spread in the neutron/seed ratio and, in turn, in [hs/lr] and [Pb/hs].

However, recent asteroseismic observations (KEPLER, TESS) show that rotation is probably suppressed in most of the giants.

A (theoretical) classification

| | Type I | Type II | Type III | Type IV | Type V | Type VI super-AGB |
|---|---------|----------|--------------------|---------------|---------------|----------------------|
| Mass range: | | | | | | |
| Disk | <1.2 | 1.2-1.8 | 1.8-3.5 | 3.5-5 | 5-8 | 8-10 |
| Halo | <1.0 | | 1.0-2.5 | 2.5-3 | 3-6.5 | 6.5-9 |
| TDU | NO | YES | YES | ? | ? | ? |
| HBB | NO | NO | NO | marginal | YES | YES |
| s-process: | | | | | | |
| $^{22}\text{Ne}(\alpha, n)^{25}\text{Mg}$ | NO | NO | marginal | YES | YES | YES |
| $^{13}\text{C}(\alpha, n)^{16}\text{O}$ | NO | YES | YES | YES | marginal | NO |
| Final core mass | 0.5-0.6 | ~ 0.6 | ~ 0.7 | 0.7-0.9 | 0.9-1.1 | 1.1-1.3 |
| C/O | 0.35 | 0.5-0.9 | 0.5 -2 0.5-1000 | 0.5 to >1 | <1 >1 | <1 |
| spectral type | M | M, MS, S | M,MS,S & C | M,MS, S &C | M,MS, S &C | M |